1963

Construction and operation of a steady state plasma study facility

Smith, Carol C.

Monterey, California: U.S. Naval Postgraduate School

CONSTRUCTION AND OPERATION OF A STEADY STATE PLASMA STUDY FACILITY

CAROL C. SMITH,
THOMAS H. EWALL
and
ROGER D. JOHNSON

CONSTRUCTION AND OPERATION OF A STEADY STATE PLASMA STUDY FACILITY

* * * * *

Carol C. Smith, Jr.

Thomas H. Ewall

and

Roger D. Johnson

CONSTRUCTION AND OPERATION OF A STEADY STATE PLASMA STUDY FACILITY

by

Carol C. Smith, Jr.
Lieutenant Commander, United States Navy

Thomas H. Ewall
Lieutenant, United States Navy

and

Roger D. Johnson
Lieutenant, United States Navy

Submitted in partial fulfillment of
the requirements for the degree of

MASTER OF SCIENCE
IN
PHYSICS

United States Naval Postgraduate School
Monterey, California

1963

CONSTRUCTION AND OPERATION OF A STEADY STATE PLASMA STUDY FACILITY

by

Carol C. Smith, Jr.
Thomas H. Ewall
and
Roger D. Johnson

This work is accepted as fulfilling
the thesis requirements for the degree of
MASTER OF SCIENCE
IN
PHYSICS
from the
United States Naval Postgraduate School

ABSTRACT

A steady-state, highly-ionized plasma system has been built for use by the plasma physics group of the Department of Physics of the U. S. Naval Postgraduate School, Monterey, California. This system will be used to study electro-magnetic, hydromagnetic, and ion waves in a plasma, and charged particle diffusion in a variable magnetic field.

The experimental tube is a nine foot long assembly of four inch diameter pyrex sections with access ports at 14 inch intervals. The continuous plasma source is a hollow cathode discharge operating in a reflex configuration using either argon or helium at a cathode pressure of approximately one micron. Differential pumping of neutral particles is utilized to give a pressure in the region of the floating anode of the order of 10^{-5} mm Hg. The discharge carries up to 200 amps at 160 volts. The longitudinal magnetic field is variable up to 10,000 gauss and is homogeneous to within 2.5% along the axis of the plasma column.

The design and details of construction of each of the components are presented along with operating characteristics and proposals for future diagnostic techniques.

The writers wish to express their appreciation of the supervision and technical advice of Professor N. L. Oleson and Professor A. W. Cooper and for the assistance of Mr. Robert Smith and Mr. Peter Wisler.

TABLE OF CONTENTS

LIST OF ILLUSTRATIONS

List of Symbols

a	Cavity radius
B	Magnetic field
C	Conductance of vacuum system component
d	Length of cavity
E	Electric field intensity
e	Charge of electron
I	Electric current
J_i	Ion current density
J_o	Zero order Bessel function
J_1	First order Bessel function
K	Bessel function constant
k	Boltzmann's constant
m	Mass of particle
m_e	Mass of electron
m_i	Mass of ion
n	Number density of particles
n_e	Number density of electrons
n_i	Number density of ions
Q	Throughput
$Q_{b\text{-veeco dp}}$	Effective throughput of baffle and Veeco diffusion pump assembly
$Q_{b\text{-cvc dp}}$	Effective throughput of baffle and CVC diffusion pump assembly
$Q_{electronic}$	Ratio of stored electric energy to dissipated electric energy
R_s	Surface resistivity
S	Pumping speed
S_p	Speed of vacuum pump
T	Absolute temperature

V	Electric voltage
W	Electric power
ϵ	Dielectric constant
η	Characteristic resistance of free space
λ	Wavelength
λ_r	Resonant wavelength
μ	Microns of pressure
σ	Collision cross section
ω	Angular frequency
ω_p	Plasma frequency

1. Introduction.

The completion of the Plasma Study Facility has provided the Physics Department of the U. S. Naval Postgraduate School, Monterey, California, with a research tool by means of which the characteristics of a highly-ionized, steady-state plasma can be studied. Reference /1/ describes this plasma study facility as originally conceived and partially constructed in the basement of Spanagel Hall. In the summer of 1962, because of inadequate space and unattainable power requirements, the facility was completely disassembled and the components moved to Building 223. From August 1962 to March 1963 the facility was reconstructed employing several changes to the original design. By March 1963 all of the components were in operation with the exception of the power supplies for the magnets. Temporary power supplies are available which are capable of supplying a magnetic field of approximately 1500 gauss. The provisions for a field of 6500 gauss should be completed by June 1963; with the purchase of additional equipment after July 1963, a field of approximately 10,000 gauss will be available.

This report presents the design, construction and operating parameters of the arc discharge; the vacuum system with its pumps, valves, electronic measuring components, and associated cooling equipment; the magnetic field, its alignment, and the associated water cooling and deionization equipment; and the design of the various diagnostic techniques. To serve as a guide and handbook for future students newly acquainted with the system, an appendix is provided containing schematics and operating check-off lists.

2. The Arc Discharge.

The plasma for the steady state column is continuously generated by an arc discharge between the gas-fed hollow cathode and the annular first anode. The plasma passes through the aperture of the first anode and fills the column as a beam down to the second or floating anode. This anode helps sustain the beam by operating the discharge in a reflex mode /1/.

The electrode configuration with respect to the vacuum system and magnet coils is shown in Fig. 1 and its electrical circuit schematic in Fig. 13b.

Fig. 2 is a drawing of the cathode assembly which follows the design used by Rose /2/. The helium or argon gas flows through several centimeters of the cathode tube of tantalum or tungsten where it is ionized by the high current discharge which runs into the interior of the tube. The highly ionized gas then leaves the cathode and forms the beam. The heat generated by the ionizing arc is removed by two means. First, the hollow cathode is mounted in a heavy copper plug by a shrunk-fit technique which assures good heat transfer from the tube to the base plug. The plug in turn is held in the cathode base which is water cooled at a flow rate of two gpm. Second, the radiant heat emitted by the arc heated cathode tube (2500-3000^{o}C) and by the arc itself is absorbed by the copper walls of the anode-cathode shell which is also water cooled at two gpm.

The cathode mechanism is believed to be as follows: the gas flowing through the cathode towards the vacuum chamber has

a negative pressure gradient in the direction of the vacuum chamber and at some distance along the tube, depending on the gas flow, a pressure (approximately one micron) suitable for the operation of an arc is reached /1/. The electrons are emitted from the inside walls of the cathode thermionically or by field emission across a very thin sheath. Those electrons that collide with gas molecules before returning to the walls are trapped and drawn out of the cathode by the axial potential gradient of the arc /3/ as well as by the pressure gradient of the plasma. This idea is supported by observation of the cathode while the arc is running. The arc appears to come from a well defined ring in the cathode which is heated intensely. The collisions of the electrons with the gas molecules produce positive ions and electrons, radiation, and possibly some metastable excited atoms. Nearly all of these products of collisions are trapped in the tube and return to the wall, heating it to a temperature of nearly 3000°C. Thermionic emission of electrons results and adds to the field emission electrons discussed previously. This plasma in the tube is of high density and is the main source for the lower density plasma in the arc and in the beam. Additional ionization takes place external to the cathode by the electron current to the first anode and by the electrons moving in a reflex mode along the beam between the first and second anodes.

An estimate of the current balance is made by Rose /2/ for a plasma with a small axial electric field and low energy losses. The assumptions are:

(1) The electron current, I_{ec}, from cathode to anode is made up of (a) I_{ec1}, electrons arriving at the anode (at applied potential V) without exciting or ionizing the gas in the cathode; (b) I_{ec2}, electrons that have ionized or excited the gas and arrive at the anode with plasma temperature T_e; (c) I_{eg}, electron current due to electrons which have been detached from gas atoms and which arrive at the anode with energy T_e; and

(2) The ion current, I_{ic}, from the ionization process.

$$I_{ic} = I_{eg} \tag{2-1}$$

Thus the current to the anode or cathode is

$$I = I_{ec1} + I_{ec2} + I_{eg} \tag{2-2}$$

and the power dissipated at the anode is

$$W_a = I_{ec1}V + (I_{ec2} + I_{eg})T_e \tag{2-3}$$

The electrons of I_{ec2} produce ionization once, but not twice, because of the competing excitation processes /2/. By definition, $\bar{\sigma_x}$ is the cross section for inelastic collisions not leading to ionization, and $\bar{\sigma_i}$ is the cross section for direct ionization plus excitation. Therefore:

$$I_{ic} = I_{eg} = I_{ec2} \,/\left(1 + \frac{\bar{\sigma_x}}{\bar{\sigma_i}}\right) \tag{2-4}$$

Combining the above equations gives

$$I_{ec} = \frac{I\left(1 + \bar{\sigma_x}/\bar{\sigma_i}\right) + \left(W_a - IT_e\right)/\left(V - T_e\right)}{2 + \bar{\sigma_x}/\bar{\sigma_i}} \tag{2-5}$$

and

$$I_{ic} = \frac{I - \left(W_a - IT_e\right)/\left(V - T_e\right)}{2 + \bar{\sigma_x}/\bar{\sigma_i}} \tag{2-6}$$

In most cases of interest, the ratio I_{ic}/I_{ec} is small, which shows that the electron current is due primarily to thermionic and field emission. A sample calculation /2/ shows that I_{ic}/I_{ec} equals 1/6 when I/I_{ic} equals $\frac{1}{4}$. Thus, each atom is ionized several times in the cathode and is neutralized several times at the cathode surface before escaping, so the probability of escaping as a neutral atom is small.

Fig. 3 is a schematic of the gas input system used both for starting and for steady state operation. The flow meter used is the Matheson 602 dual float flowmeter with a range of 110 to 1760 atm-cc/min. A copper coil immersed in liquid nitrogen serves as a cold trap when running on helium. For continuous operation on argon, acetone and dry ice would be used as the cooling agent.

The operating gas is supplied from a four foot diameter meteorological balloon inflated to approximately atmospheric pressure. This provides a constant-pressure, fluctuation-free gas supply. During early runs on argon and helium, using only the tanks and pressure regulators, arc pulsations occurred, which are believed to be due to the chattering of the pressure regulator. Similar pulsations have been observed using the balloon supply when the flow rate establishes the resonant frequency of the ball float in the meter.

To start the arc, the check-off list in Appendix A-II should be followed, because improper sequencing may result in the destruction of electrodes and meters, the loss of the vacuum within the column, or inability to initiate the arc.

The actual start is as follows: with proper cooling flows, cathode magnets and main field on, and the two arc power supplies at maximum voltage (170V), the RF starter is turned on to supply the initial breakdown energy to the gas. The purpose of the boron nitride shield now becomes apparent. A start is impossible if the shield is not in place because the RF intensity is reduced. If the cathode material has plated out on the shield face, a low-resistance RF path results, so that a start is again impossible. The latter situation has been corrected by making an annular undercut groove of one and 20/32 inch diameter around the cathode hole in the boron nitride shield. A burst of argon gas is then admitted, the arc starts, and the argon flow is reduced. This method, as opposed to a gradual increase of flow until starting, gives quicker starts and at the same time prevents loading the vacuum system with neutral gas. If argon is the operating gas, the RF may then be turned off. At the same time, the plasma in the arc between the cathode and first anode is observed to move through the orifice of the anode and fill the column with an intense blue-white beam characteristic of argon. This occurs as the vacuum system pumps away the initial un-ionized or ionized-and-recombined neutrals of the starting burst, so that the system base pressure diminishes and develops a neutral pressure gradient along the column of from 10^{-3} mm Hg at the cathode to 10^{-5} mm Hg at the floating anode. The arc voltage and gas flow are then adjusted to give the desired beam and current.

If helium is to be the operating gas, the start is made on argon. After the beam is established, the argon is valved off while the helium is turned on. This transition takes a few seconds and requires an increase of the external resistance and an increase of the arc voltage to its maximum, because of the higher ionization potential of helium (He - 24.46ev, A - 15.68ev). The transition is readily observable in the arc as a smooth shift in color and intensity from the blue-white of argon to the less intense reddish-orange or "dusty peach" of helium. This shift of color and intensity then occurs throughout the column. The voltage, external resistance, and gas flow may be adjusted over a fairly wide range for continuous operation.

Initial starting on pure helium has been attempted many times, utilizing varying combinations of the previously mentioned parameters with little success. In one of these attempts the plasma beam started down the column in what may be described as a slow-moving fireball. It reached the floating anode, returned to the first anode, and extinguished the arc. This result was reproduced on several tries, but no sustained operation was achieved. On another occasion, a very small cathode (.166" ID) was used, and the arc and beam established; however, the current flow was so high that the cathode melted in about one minute.

The value of using the RF starter while transitioning is as yet undetermined. It appears to aid when transitioning with the large (.460 " ID) cathode, while definitely inducing

instabilities in the small cathode (.296" ID). Why it should not aid the transition in all cases poses an interesting question.

The duration of operation of the plasma column in a steady state, or continuous mode, has ranged from as long as one hour to as little as five minutes. The continuous operations were limited by the heating of the glass section surrounding the first anode, and to some extent by the heating of the glass section surrounding the floating anode. Temperatures of 350°C were recorded on the surface of the glass surrounding the first anode. The glass has been replaced by a water cooled copper shell with four inch viewing ports. The heating problem in the floating anode area has been solved by replacing the glass with an equivalent stainless steel section.

Table 1 contains some characteristic data taken during steady state operation. The floating anode pressures are order of magnitude only, because maintenance of a reliable vacuum gauge amplifier was difficult.

Neigdigh and Weaver /4/ describe two distinct modes of operation for a hollow cathode discharge. Mode I has clearly defined beam edges with uniform brilliance along the entire beam length and a characteristic color associated with the gas being used. This mode requires a pressure of one micron and no gradient. Mode II occurs when increased pumping is applied to the system operating in Mode I, developing a gradient along its length. The arc transitions to a mild glow and the beam diminishes along its length.

In both modes, the floating anode assumes a negative potential with respect to the first anode of nearly double the anode to cathode, or arc, potential. Both modes of operation have been observed in this column, but with two disparities. First, both modes exist with pressure gradients present; the first mode being observed with the large diameter cathode and the second with the small diameter cathode in use. Second, whether large or small diameter cathodes are used, the floating anode is only some tens of volts below the first anode, rather than some hundred to two hundred volts below it.

A major problem yet unsolved in the steady state operation of the discharge is the brief cathode operating life. The maximum operating lifetime on any of the eight cathodes used to date has been two hours. Rose /2/ reports lifetimes of many hours at several hundred amperes. Reports from the Plasma Group at Berkeley /5/ indicate lifetimes of approximately one hundred hours, but at lower currents than reported by Rose. Two definite criteria exist for sustained discharge operation. First, the length to ID ratio must be six to one or greater to obtain the necessary pressure gradient and associated hot spot for proper ionization of the gas. Second, the heat generated by the arc must be removed either by making the cathode wall thin enough to permit the radiation of the absorbed energy /2/, or by enclosing the entire cathode in a water cooled copper jacket for sufficient heat transfer as done by Luce /3/. Various combinations of ID and wall thickness are being investigated.

The size of the arc is determined by the inside diameter of the cathode and by the applied cathode magnetic field. Varying the field up to 900 gauss does not change the arc size appreciably; however, increasing the field does increase the definition of the arc boundary. The size of the beam in the column is determined by the size of the aperture in the first anode, and by the main magnetic field. Increasing the main field decreases the beam size and increases the boundary definition.

Gas	Flow Rate Atm-cc/min	Arc Voltage (cathode to anode) (volts)	Arc Current (amps)	Floating Anode Potential (volts)	B Field Current Kilogauss	Neutral Cathode	Pressure (mm Hg) Floating Anode	Cathode (Tantalum) all dim. in inches Length	I. D.	Wall Thickness
He	425	143	73	63	250 amp 1.5	10^{-3}	3×10^{-4}	3.5	0.46	0.020
He	425	112	92	68	250 amp 1.5	10^{-3}	3×10^{-4}	3.5	0.46	0.020
He	425	100	75	78	250 amp 1.5	4×10^{-3}	9×10^{-4}	3.5	0.46	0.020
He		80	150	-	250 amp 1.5	10^{-3}	3×10^{-4}	3.0	0.296	.079 cathode lasted 30 sec
He	200	60	10	-	280 amp 1.68	10^{-3}	4×10^{-4} system had leak	2.25	.296	.079
He	200	83	18	34	260 amp 1.55	10^{-3}	4×10^{-4} system had leak	2.25	.296	.079

Table 1

3. Magnetic Field.

Design and Specifications: The design of the coils and cooling system to provide an axial magnetic field variable to 10,000 gauss and capable of continuous operation was undertaken by Professor A. W. Cooper of the Physics Department of USNPGS. Although an axial field variation of less than one percent was originally desired, a variation of less than $2\frac{1}{2}$ percent was accepted because of economic considerations. The specifications to meet these standards were determined and the contract was awarded to the Pacific Electric Motor Company of Oakland, California. The magnets were received in October 1962.

Each magnet consists of 15 layers of 12 turns each. The conductors are .640 inch square copper tubes with a .402 inch circular bore, enabling the conductors to serve also as cooling water conduits. The conductors are insulated by mylar tape and the assembly is set in epoxy resin. The six main magnets have an 18 inch bore and 39 inch outside diameter while the mirror magnet has a ten inch bore and a $31\frac{1}{2}$ inch outside diameter. In addition, a small magnet which surrounds the arc discharge cylinder was made locally.

The axial field was measured utilizing a Halltron (HP-315) axial field probe. The results are plotted in Fig. 4 under a schematic showing the magnet dimensions and spacing. The six large magnets and the mirror magnet are supplied in series. The mirror magnet can be separately supplied to vary the mirror ratio. The results shown are with the small cathode magnet supplied with a current of 120 amps. The field is completely

uniform radially within the pyrex tube. The maximum spatial variation of the axial field between magnets 2 and 5 is less than 2.5 percent.

Alignment Procedure: The geometric axes of discharge vessel and coil system were first adjusted to coincidence visually. The linearity of the magnetic field and the parallelism of the discharge tube axis and magnetic field lines were tested with a thin electron beam. This beam was observed with electrostatic probes and optically by the light emitted in excitation of residual gas atoms. When the alignment was completed, it was considered that the axes coincided within one millimeter throughout the length of the column.

Magnet Power Supply: Fig. 5 is a schematic of the proposed power supply for the magnetic field. The shed to house the components is presently being constructed adjacent to Bldg. 223. When completed, this supply will provide a magnetic field which is variable up to 10,000 gauss with a field of approximately 11,500 gauss in the vicinity of the mirror coil.

The 4160 volt, three phase, 60 cycle supply voltage is stepped down through six parallel-delta-connected transformers which supply, through a distribution board, ten 40 volt 1700 ampere Airco selenium rectifiers. Nine of these rectifiers are connected in series to supply the six main magnets and one is used to supply the mirror coil. The total series resistance at room temperature of the six main coils is .26 ohms and the resistance of the mirror coil is .031 ohms.

While awaiting the completion of this power supply system, two Plasmatron rectifiers capable of supplying 250 amperes have been used for the magnets. This limits the longitudinal field to approximately 1500 gauss. A schematic of this temporary power supply is contained in Fig. 13a.

Magnet Cooling System: A schematic of the cooling system is shown in Fig 6 and a photograph of the components which are mounted on a concrete pad outside of Building 223 is contained in Fig. 14. The system was designed to give a maximum cooling rate of 500 kilowatts with a flow rate of 120 gallons per minute. The cooling water is recirculated for reasons of economy and purity. The magnet cores are cooled by deionized water at a maximum inlet pressure of 90 psi and the heat dissipated in the heat exchangers. The heat absorbed by the raw water in the heat exchangers is released in the cooling tower. The deionizers decrease the specific conductivity of the cooling water from 40 micromhos/cm to less than one micromho/cm. A list of the system components with their performance data is included in Appendix D.

4. Vacuum System.

The vacuum chamber or column which provides a sufficiently low neutral gas pressure to permit the formation of an arc discharge and its associated plasma beam is shown in Fig. 1 and Fig. 14. The chamber is an assembly of standard four inch Kimax tempered glass (pyrex) pipe sections in 12 or 14 inch lengths of straight, tee, or cross form. The sections are joined to each other, the cathode-anode shell, or to the diffusion pump riser pipe flanges by bolting together the aluminum flange and backing ring insert combinations. The sealing of the component sections of the system is by O-rings (Buna N or Viton in high temperature areas) properly cleaned, greased and wiped off.

The diffusion pumps are mounted on legs adjustable as to position and height so that the column may be properly aligned with the magnetic field (alignment procedure is described in Section 3). A schematic of the vacuum system components is shown in Fig. 12 and its protective interlock features described in Appendix B.

The vacuum system was designed /1/ to maintain an operating pressure of from one to ten microns in the region of the discharge, decreasing down the length of the column to approximately 10^{-5} mm Hg in the region of the floating anode. These pressures are maintained by differential pumping due to the system configuration, while maintaining a throughput of approximately 1500 micron-liters/sec (118 atm-cc/sec). The 2.8 cu. ft. system can be pumped down from atmospheric pressure to 10^{-6} mm Hg in one hour and 10^{-7} mm Hg in three hours. The system has the very attractive feature of being readily disassembled

and reassembled in order to provide nearly any desired access port arrangement for diagnostic instrumentation. All the glass sections are wrapped in fiber glass cloth and impregnated with epoxy resin to reduce flying splinters in the event of an implosion.

The system components with specifications, and the throughput calculations for the system with their resulting system pressures are shown in Appendix C. A summary of these results for the various throughputs is as follows:

(present configuration)

Q = 5000 micron-liters/sec, system pressure three microns

Q = 2520 micron-liters/sec, system pressure one micron

(with an additional booster)

Q = 10,000 micron-liters/sec, system pressure 12 microns

Q = 5400 micron-liters/sec, system pressure four microns

The throughput calculations for an additional booster were made in anticipation of its installation during the summer of 1963.

A summary of actual throughputs (air and helium) and their respective system pressures both with and withough the discharge is shown below.

Table 2

Without discharge

	Air	Helium (corrected ion gauge readings)
Q=2520 micron-liters/sec (200 atm-cc/sec)		
Pressure in system at:		
cathode thermocouple	0 microns	0 microns
foreline thermocouple	23 microns	19 microns
first anode ionization gauge	3.8×10^{-4} mm Hg	9.8×10^{-4} mm Hg
floating anode ionization gauge	7.0×10^{-5} mm Hg	3.0×10^{-4} mm Hg
Q=5400 micron-liters/sec (425 atm-cc/sec)		
Pressure in system at:		
cathode thermocouple	0 microns	0 microns
foreline thermocouple	25 microns	22 microns
first anode ionization gauge	7.0×10^{-4} mm Hg	1.8 microns
floating anode ionization gauge	1.2×10^{-4} mm Hg	3.8 microns

5. Diagnostic Techniques.

Theory of Probes: Langmuir-type probes consisting of small cylindrical electrodes to which various potentials may be applied and corresponding currents measured, have been used in plasmas to obtain information on electron temperature, ion and electron densities, and space potential. An outline of the conventional probe theory for measurements in the absence of a magnetic field (due to Langmuir /18/) and a discussion of the effect of strong magnetic fields is given below:

Fig. 7 is a somewhat idealized plot of the measured current versus potential applied to the probe. As the probe potential is increased from a large negative value, through zero to a positive value, the probe current changes radically as depicted in the plot. At the extreme left, with the probe sufficiently negative with respect to the plasma, the probe will accept only positive ions. The constant current along AB is called the random ion current, I_{ri}, and is proportional to the ion density. As the probe potential becomes less and less negative and eventually positive, the probe is able to accept more and more electrons and the current changes from B to C. At point C there are equal numbers of electrons and singly-ionized positive ions arriving at the probe causing the net current to be zero. The potential of the probe at point C is called the "floating potential", because it is that potential assumed by the probe when allowed to float electrically. Further increase of probe potential leads to a rapid rise in negative currents collected until the point D is reached. At

point D the electrons reach the probe at their maximum rate, determined by the electron density of the plasma, and the current becomes constant even though the potential of the probe is increased. The probe potential at point D is called the "space potential". Beyond D there is a negligibly small collection of positive ions due to their small energy spread and the repulsive potential of the probe. The difference in the current at D and the random ion current is called the random electron current, I_{re}.

Between points C and D the number of electrons reaching the probe exceeds the number of positive ions and a negatively charged sheath surrounds the probe repelling those electrons with insufficient energy to penetrate the sheath and reach the probe. The electron current, I_e, for any applied potential (for example, point P) is proportional to the electron density at the surface of the probe. Assuming a Boltzmann distribution, the electron current to the probe is:

$$I_e = I_{re} \exp(- eV/KT_e) \qquad (5\text{-}1)$$

where T_e is the plasma electron temperature and V is the potential across the sheath. At point D, I_e equals I_{re} since the potential across the sheath has been decreased to zero. Above point D all electrons reaching the sheath are able to penetrate to the probe and contribute to the electron current. From equation 5-1, since I_e and I_{re} can be obtained experimentally, it is possible to obtain the electron temperature, T_e, if the potential difference across the sheath, V, is known. As stated above, the value of V at point D is zero. If the

applied probe potential at point D is V_d then V at any point can be expressed as $V_c - V_p$ where V_p is the applied probe potential at that point. Replacing V by $V_c - V_p$ in equation 5-1 and taking the logarithm of both sides one gets:

$$\text{Log}_e I_e = \text{Log}_e I_{re} - \frac{eV_d}{kT_e} + \frac{eV_p}{kT_e}$$

$$= \text{constant} + \frac{eV_p}{kT_e} \qquad (5\text{-}2)$$

From the slope of a semi-log plot of equation 5-2 one can obtain a value of T_e.

For a Maxwellian distribution of particles, it can be shown by kinetic theory that the rate at which particles strike a unit area is equal to $n(\frac{kT}{2\pi m})^{\frac{1}{2}}$ particles per second. Therefore the random electron current to a probe of area A is:

$$I_{re} = Aen_e(\frac{kT_e}{2\pi m_e})^{\frac{1}{2}} \qquad (5\text{-}3)$$

If the electron temperature is obtained from the semi-log plot described above, the density of electrons, n_e, can be determined from equation 5-3 since all other quantities are known.

The above derivations are valid so long as the probe radius is very much smaller than the mean free path of the particles. This condition is met for both ions and electrons in the absence of a magnetic field. When a magnetic field is applied, however, the effective mean free path of the particles is reduced to the order of the radii of their respective Larmor orbits. For a field of the order of one kilogauss the effective mean free path for electrons becomes less than the

applied probe potential at point D is V_d then V at any point can be expressed as $V_c - V_p$ where V_p is the applied probe potential at that point. Replacing V by $V_c - V_p$ in equation 5-1 and taking the logarithm of both sides one gets:

$$\text{Log}_e I_e = \text{Log}_e I_{re} - \frac{eV_d}{kT_e} + \frac{eV_p}{kT_e}$$

$$= \text{constant} + \frac{eV_p}{kT_e} \qquad (5\text{-}2)$$

From the slope of a semi-log plot of equation 5-2 one can obtain a value of T_e.

For a Maxwellian distribution of particles, it can be shown by kinetic theory that the rate at which particles strike a unit area is equal to $n(\frac{kT}{2\pi m})^{\frac{1}{2}}$ particles per second. Therefore the random electron current to a probe of area A is:

$$I_{re} = Aen_e(\frac{kT_e}{2\pi m_e})^{\frac{1}{2}} \qquad (5\text{-}3)$$

If the electron temperature is obtained from the semi-log plot described above, the density of electrons, n_e, can be determined from equation 5-3 since all other quantities are known.

The above derivations are valid so long as the probe radius is very much smaller than the mean free path of the particles. This condition is met for both ions and electrons in the absence of a magnetic field. When a magnetic field is applied, however, the effective mean free path of the particles is reduced to the order of the radii of their respective Larmor orbits. For a field of the order of one kilogauss the effective mean free path for electrons becomes less than the

dimensions of any practical probe and the theory developed above is no longer valid. The ions, however, have a much larger radius which is of the order of practical probe radii.

For cylindrical probes drawing orbital-motion-limited currents, Langmuir and Mott-Smith /19/ developed the following relation for sufficiently negative voltages:

$$\frac{dJ_i^2}{dV_p} = \frac{-2e^3}{\pi^2 m_i} n_i^2$$

where J_i is the ion current density and m_i is the mass of the ion. Therefore the ion density, n_i, is proportional to the square root of the slope of the plot of I^2 versus V_p for large negative voltages with respect to the plasma potential.

Fig. 8 shows a sketch of the type of probe used locally to obtain plasma measurements. The diameter of the cylindrical tungsten tip is approximately .010 inches.

Rotating Probe: A rotating probe scheme, similar to that used in P-4 /20/ is presently envisioned as one means for obtaining information on electron temperature, ion density, and plasma potentials. Since the electron temperature is probably several electron volts, and there exists the possibility of the system containing "hot ions", such a device is deemed necessary so that the characteristics may be investigated completely through the plasma, without melting the probe. The probe will be operated in a "duty cycle" fashion with measurements taken every third or fourth pass, the remaining passes being used to allow the probe to cool (at its floating potential). In obtaining a voltage-current plot, the potential will be applied to the probe only during a time period much less than that re-

quired to rotate the probe through the plasma, so that relatively discrete points in the plasma will be obtained. By varying the time at which the probe potential is applied, the entire plasma cross-section characteristics may be investigated. The general characteristics of the housing, probe and rotator mechanism is as follows:

A. A stainless steel section is to be used to house the probe, rotating mechanism, and necessary seals. It was felt that the four inch access ports available in the glass pipe would not provide sufficient space in which to install the necessary components; thus a stainless steel section is envisioned which will replace one glass pipe section. The stainless pipe will be a four inch circular section, longitudinally, but will have an appropriately enlarged transverse "view port" section in order to house the probe, rotator, etc. The enlarged section dimensions will be limited only by the main field coil inside diameter, and by the six inch space between the coils.

B. The probe head, gearing mechanism and associated support members are to be attached to a one inch circular support cylinder, which will be sealed (by a Wilson seal) to the mounting port flange plate. The support cylinder will, in turn, contain a rotating seal where the $\frac{1}{4}$ inch stainless steel driving shaft enters the vacuum chamber. The support cylinder will be adjustable in the transverse direction, so that the

actual probe tip may be positioned with respect to the plasma. The rotating seal is similar in design to the CVC Type SR-25 and is of local design and manufacture.

C. A fractional HP d-c variable-speed motor will be used to drive the shaft at 300 rpm. A set of miter and bevel 90° three-to-one gears will be used to convert the drive shaft motion to a transverse rotary motion which will drive the probe through the plasma in a transverse plane. The three-to-one gear ratio was selected so that a low shaft speed could be used to reduce seal wear while rotating the probe through the plasma at a sufficiently high speed to prevent probe melting.

D. The probe itself will be of the conventional Langmuir design, and will utilize a boron nitride shield, both to shield all but the probe tip from the plasma, and to provide a means for attaching the probe to the revolving rotator hub by means of three screws. Probe replacement will be made through a view port on the opposite side of the column from the rotator mechanism, hence the rotator support cylinder and driving mechanism need not be disturbed for a routine probe replacement. Electrical connection to the probe hub will be through a spring-loaded pickup which rides on the hub axle. The conductor will be led out of the vacuum chamber through a Kovar seal in the flange plate.

The timing of the applied probe potential will be accomplished by mounting a mirror on the rotating shaft. Light focused on the mirror and reflected onto a photo diode will trigger an electronic counter which will also be used to apply a potential to the probe during an active pass. The various points through the plasma may be sampled by using a suitable time delay.

Microwave Electron Density Measurements: As a method of correlating probe data, a microwave technique was planned. The effect of a plasma in a microwave cavity is to change the resonant frequency of the cavity. Thus by measuring this frequency shift it is possible to determine the plasma density. A cylindrical TM_{01} mode cavity with holes in the end plates is used. This mode permits a plasma beam of at least one half the cavity diameter to be admitted coaxially. Such a situation is ideal since the cavity E field is everywhere parallel to the axis of the cavity and therefore parallel to the confining B field of the plasma beam. This permits the frequency shift to be independent of the confining B field. (The cavity B field is concentric with the cavity walls and axis.) The plasma is admitted through the holes in the flat ends of the cavity while cavity power loss is kept low by fitting on these holes short sections of circular wave guides which are below cutoff at the frequency of the cavity. See Fig. 10. This also prevents the excitation of higher modes since these guides are not below cutoff for higher resonant frequencies /7/.

X band (λ = 3 cm) was used since this frequency range permits measurements of the highest densities possible with the components readily available at this time. From microwave theory the following formulas are used to determine the ideal TM_{01} mode cavity parameters.

1. For cavity resonance the cavity radius is

$$a = \frac{\lambda r}{2.61} = \frac{3 \text{ cm}}{2.61} = 1.15 \text{ cm} \qquad (5\text{-}4)$$

where λ_r is the resonant wave length and a is cavity radius.

2. The $Q_{electronic}$ is defined as the half power width of the resonance, with the only power loss being the conduction losses of the walls.

$$Q_{electronic} = \frac{\eta}{R_s} \frac{2.405}{2(a/d + 1)} \qquad (5\text{-}5)$$

where η = 377 ohms, a as before, d is cavity length, and R_s is the surface resistivity of the walls.

$Q_{electronic}$ = 4500.

3. The frequency shift due to the presence of a medium with dielectric constant ϵ in the cavity is

$$\frac{\Delta\omega}{\omega} = \frac{\frac{1}{2} \int_D (1-\epsilon) E^2 \, dv}{\int_c E^2 dv} \qquad (5\text{-}6)$$

where E is the cavity electric field and the volume integrals are over the dielectric and cavity respectively.

4. The radial distribution of electric field in the resonant cavity is

$$E = E_o J_o(2.405 \, r/a) \qquad (5\text{-}7)$$

Solving 5-6 and 5-7 one gets:

$$\frac{\Delta\omega}{\omega} = \frac{1}{2} \frac{\int_0^R (1-\epsilon) E^2 2\pi r\, dr}{\int_0^a E^2 2\pi r\, dr}$$

$$= \frac{1}{2} \frac{(1-\epsilon) \int_0^R r J_0^2(Kr)\, dr}{\int_0^a r J_0^2(Kr)\, dr}$$

where K = 2.405/a and R is the radius of the dielectric. This gives:

$$\frac{\Delta\omega}{\omega} = \frac{1}{2} (1-\epsilon) \frac{R^2}{a^2} \frac{J_1^2(KR) + J_0(KR)}{J_1^2(Ka)} \quad (5\text{-}8)$$

Now for the cavity E field parallel to the confining B field and with the collision frequency small compared to the microwave frequency, ω, the effective dielectric constant of the plasma is:

$$\epsilon = 1 - \frac{\omega_p^2}{\omega^2} \quad (5\text{-}9)$$

where ω_p is the plasma frequency /8/ and

$$\omega_p^2 = \frac{n_e e^2}{m_e \epsilon_0} \quad (5\text{-}10)$$

$$\omega_p = 56.4\, n_e^{1/2} \text{ rad/sec} \quad (5\text{-}11)$$

with n_e in electrons/meter^3.

Solving 5-8 and 5-11 for n_e gives:

$$n_e = 6.3 \times 10^{-4} \omega \Delta\omega \frac{a^2}{R^2} \frac{J_1^2(Ka)}{J_1^2(KR) + J_0^2(KR)} \quad (5\text{-}12)$$

The cavity to be used for the density measurements is shown in Fig. 10. The two sections were turned out of brass stock and then silver-soldered together. The cavity coupling hole was then drilled and the X band wave guide silver-soldered in position. The wave guide is mounted in a brass access port plate at the proper length to place the cavity on the plasma beam axis. A thin sheet of phenolic cemented over the first wave guide joint provides the vacuum seal without appreciable attenuation of the microwaves. The measuring system is driven by a backward-wave oscillator and a modulator. The output passes through the frequency meter, a pair of directional couplers placed back to back, and into the cavity. A pair of matched crystals in the directional couplers detects the incident and reflected energy of the cavity. The ratio of these energies is compared in and displayed by the ratio meter. Thus the resonant frequencies of the cavity with and without the plasma can be determined. Prior to the actual density measurements, a dielectric rod with a diameter equal to that of the plasma beam should be slowly inserted into the cavity while measuring the frequency shift. From this procedure an $(\text{E field})^2$ versus axial distance plot can be made and the area under the curve integrated. The ratio of the integrated area between the cavity boundaries to the total area is then determined. This ratio is then the proportion of the frequency shift occurring in the cavity. This correction is applied to the frequency shift observed with a plasma and the resulting $\omega\Delta\omega$ is used in equation 5-12 to determine the electron density. A schematic

of the microwave system is shown in Fig. 11. This system is limited to measuring densities in the 4 x 10^9 to 10^{12} electrons/cc range /7/.

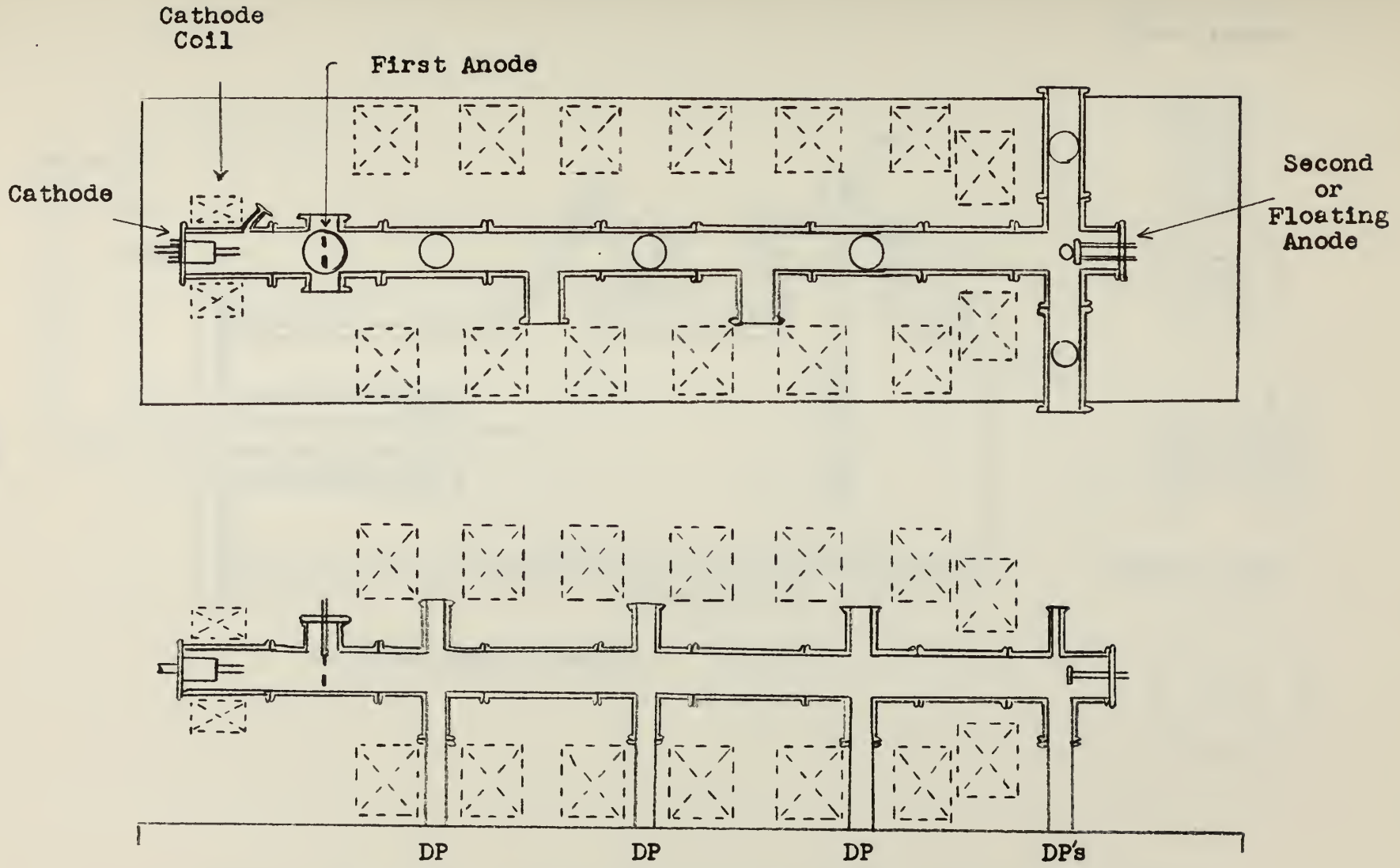

Fig. 1 Two Views of Electrodes, Vacuum Chamber and Field Coils

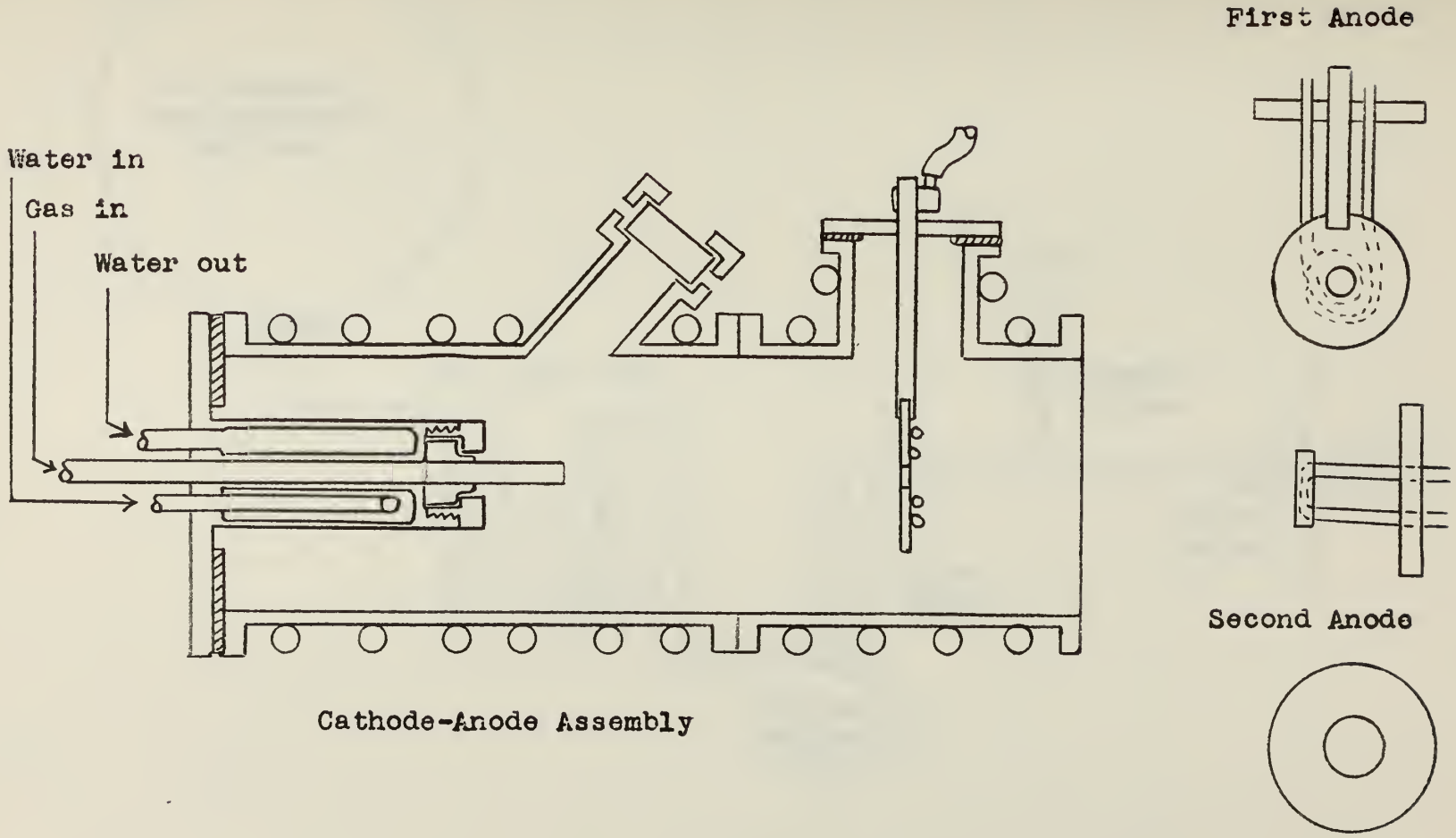

Fig. 2 Cathode-Anode Assembly and Views of First and Second Anodes

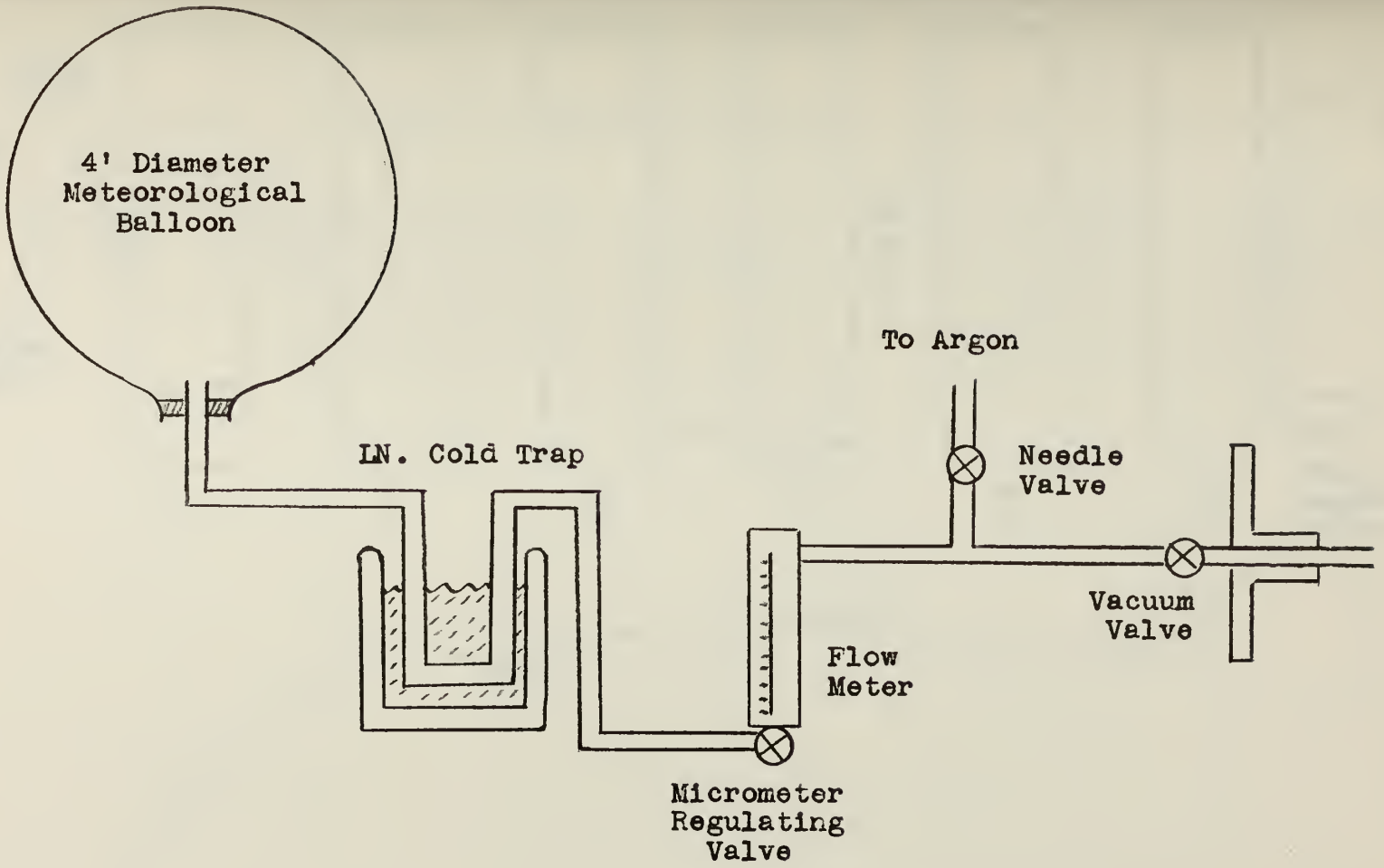

Fig. 3 Gas Input System

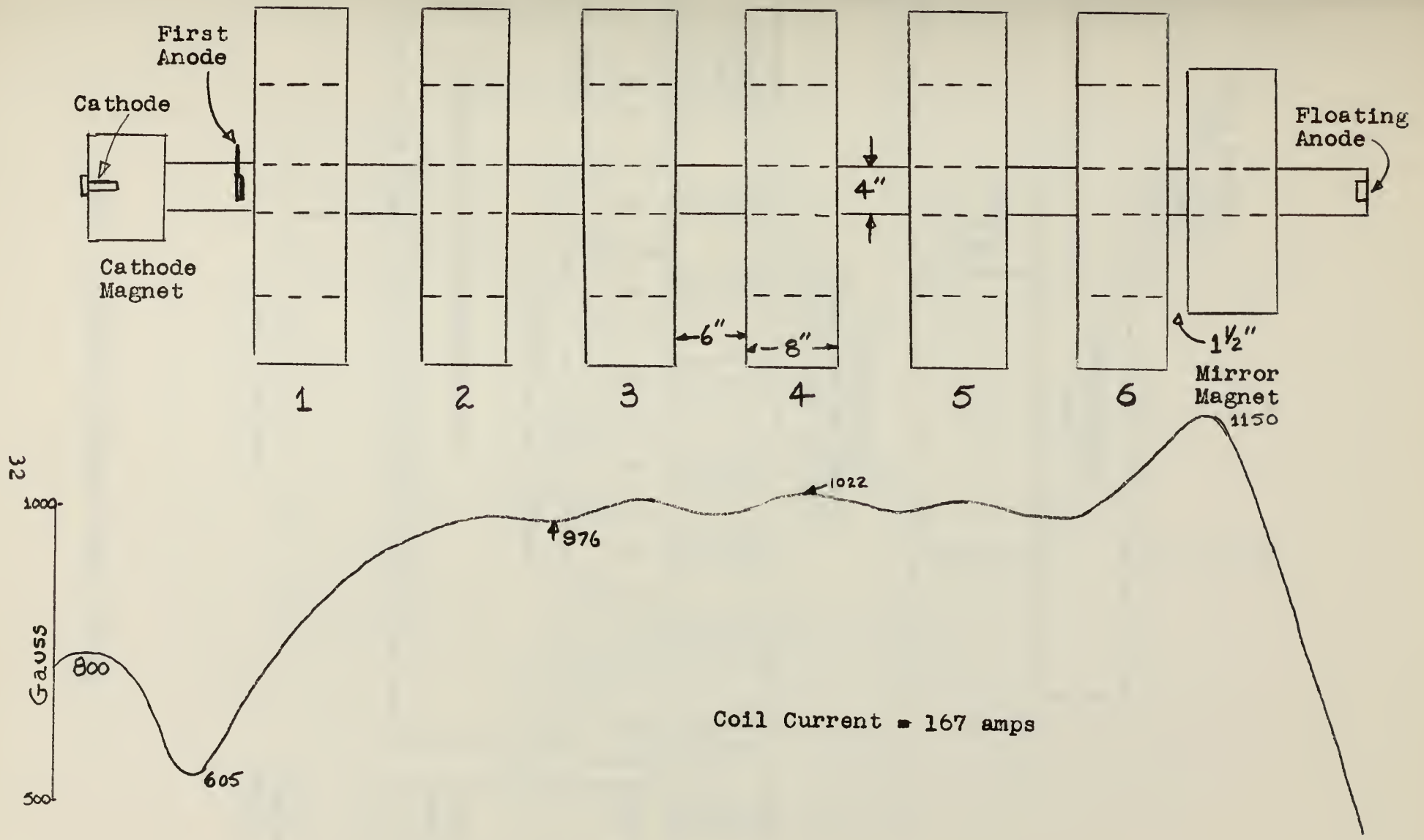

Fig. 4 Axial Magnetic Field Plot

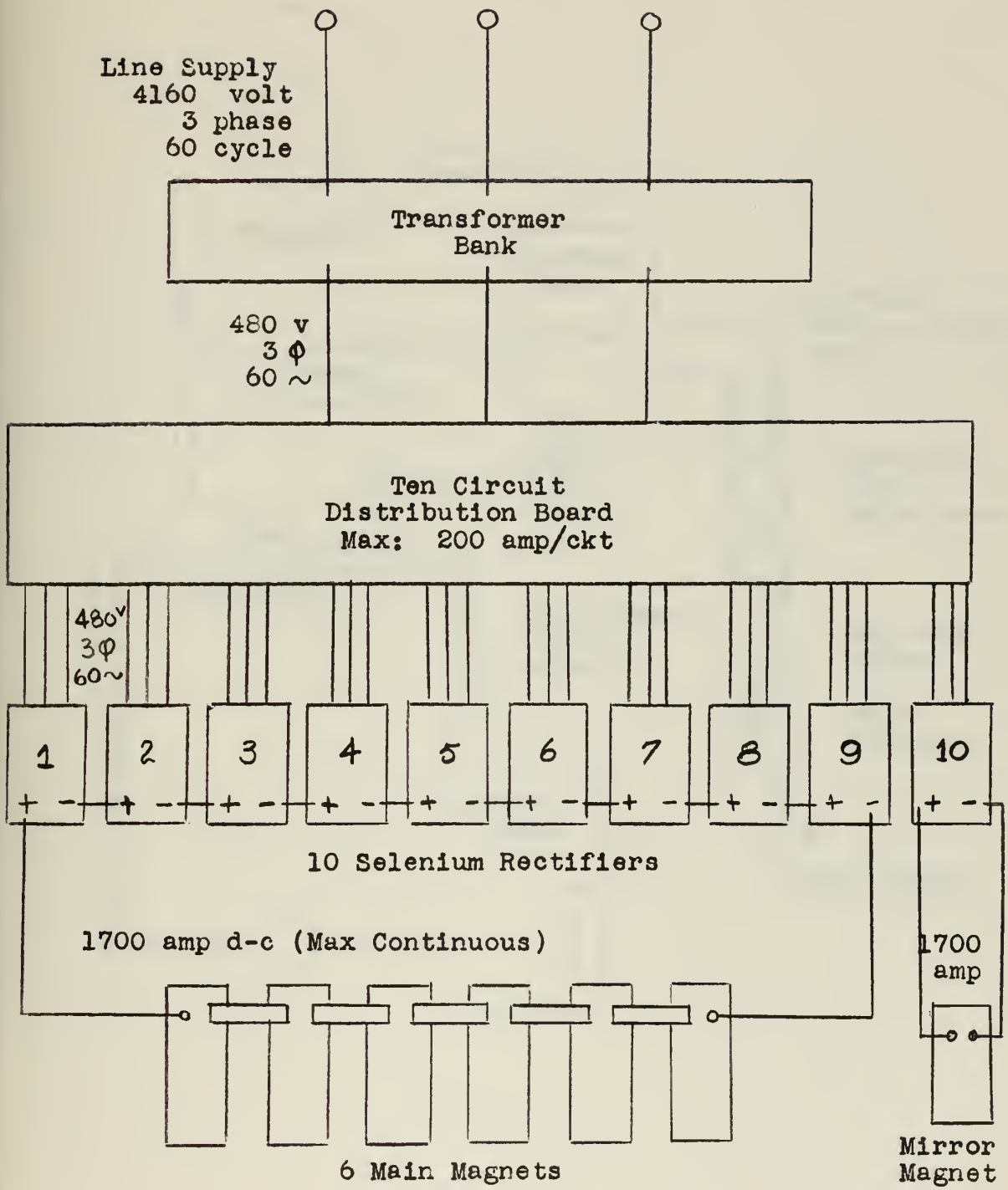

Fig. 5 Proposed Magnet Power Supply

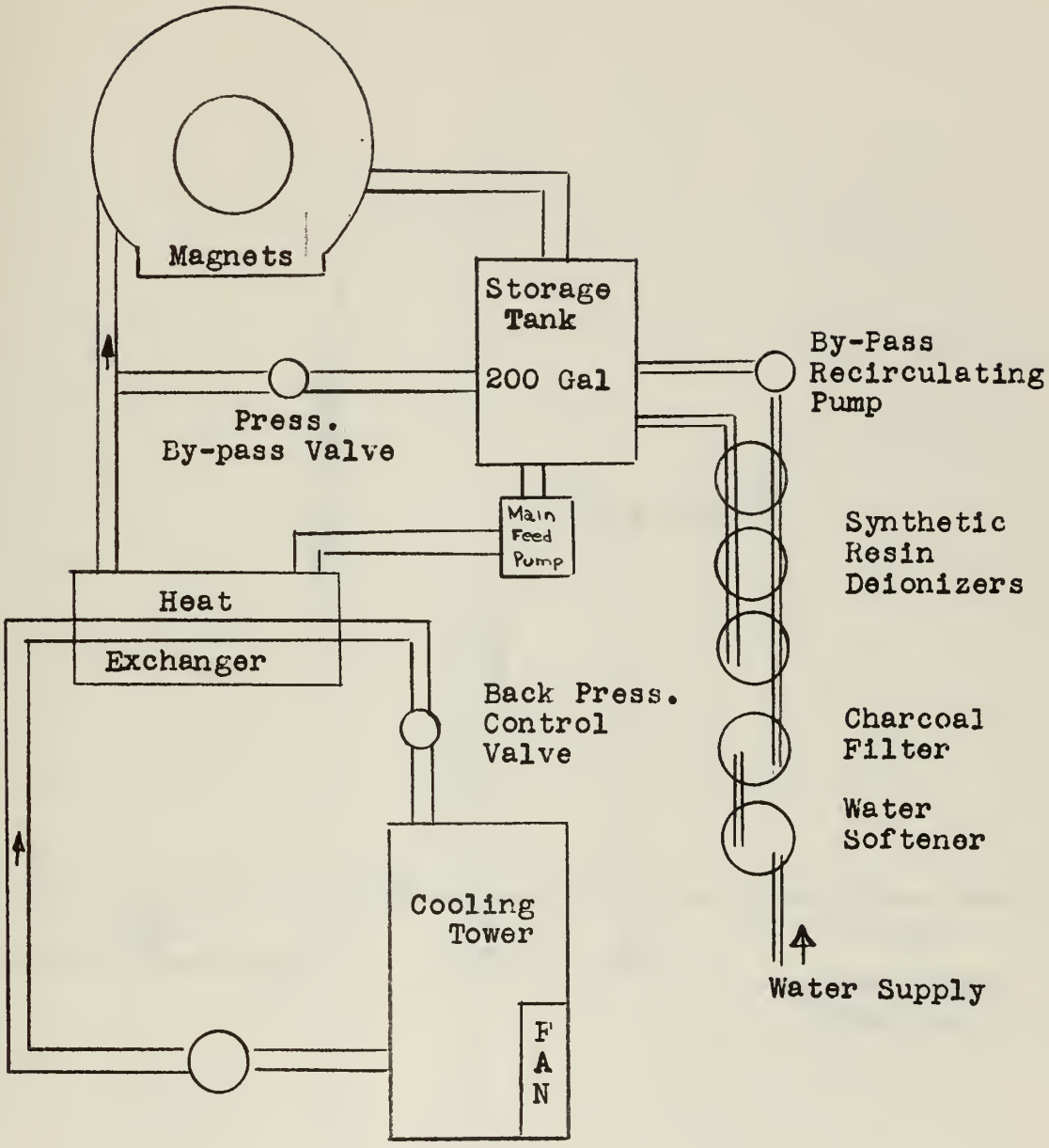

Fig. 6 Schematic of Magnet Cooling System

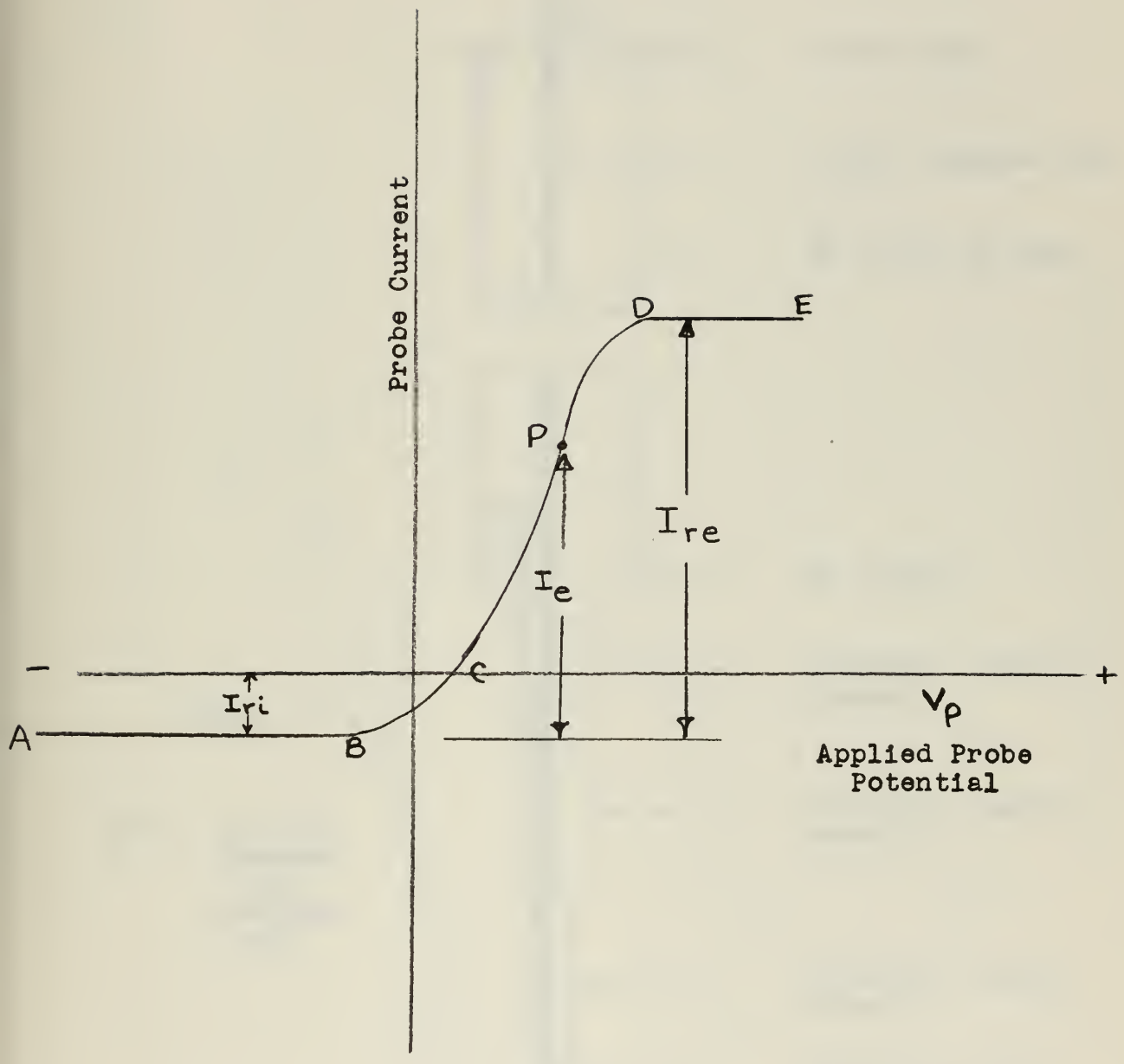

Fig. 7 Idealized Probe Characteristic Curve

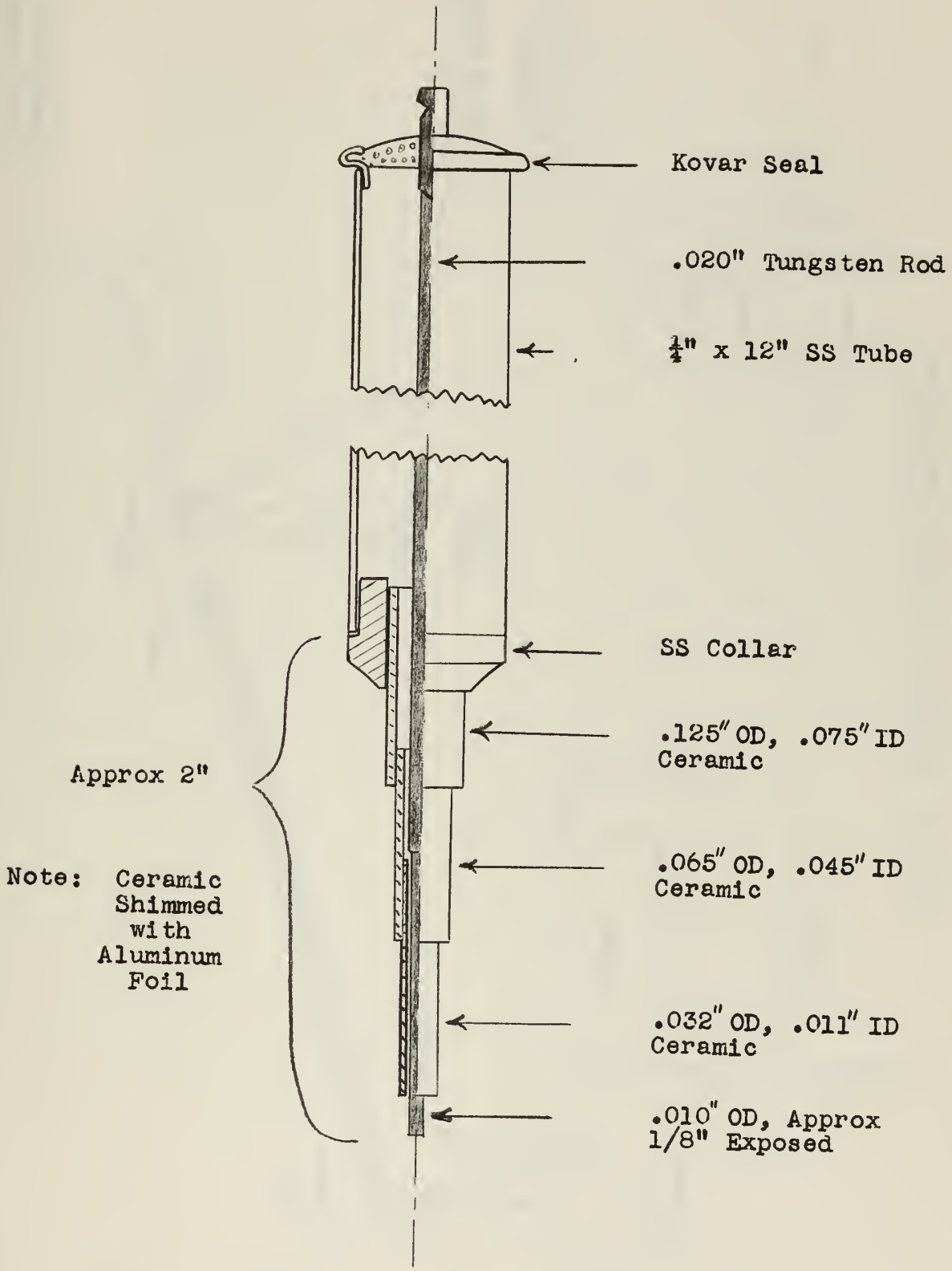

Fig. 8 Detail of an Electrostatic Probe

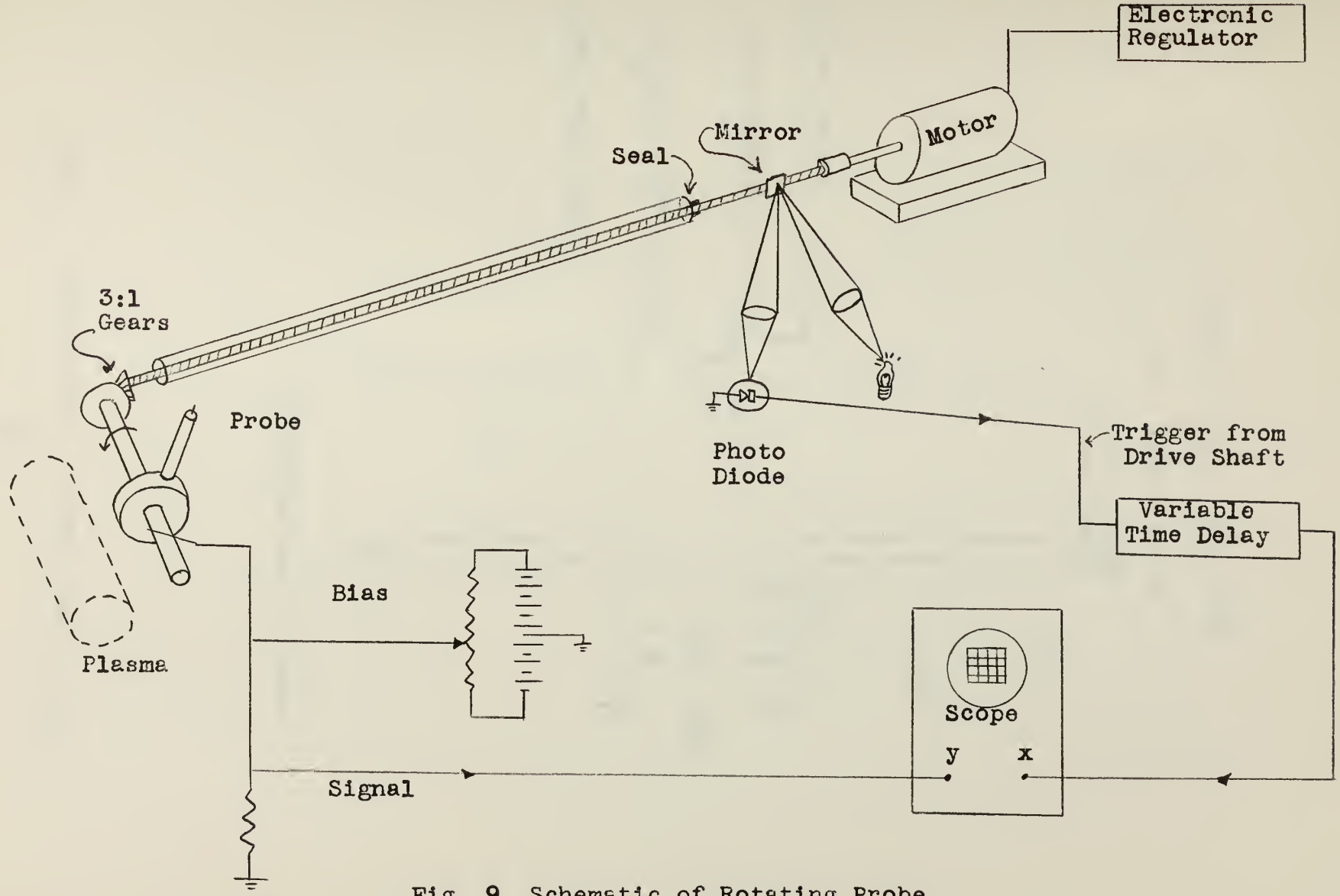

Fig. 9 Schematic of Rotating Probe

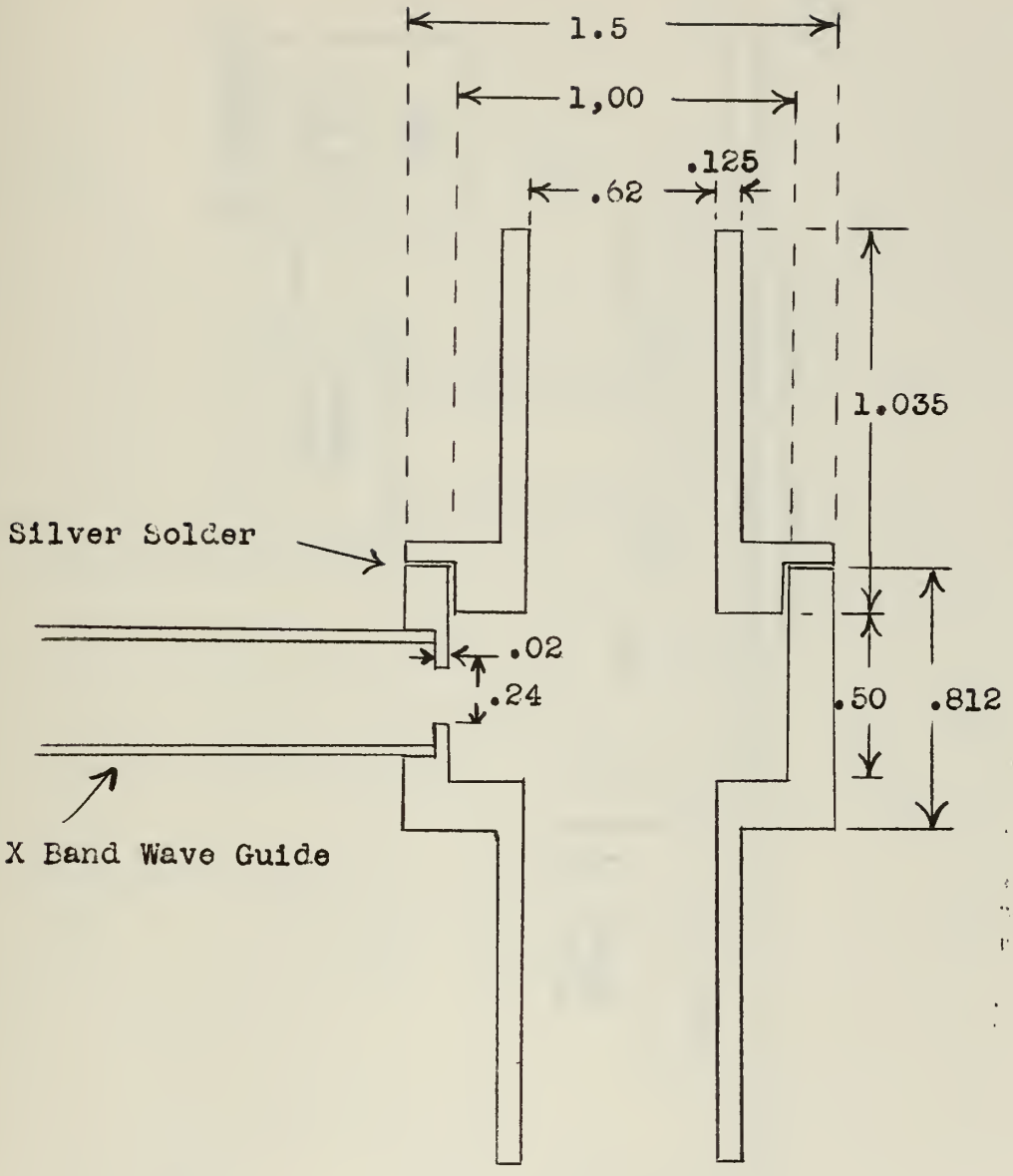

All dimensions in inches

Fig. 10 Cross-section of Microwave Cavity

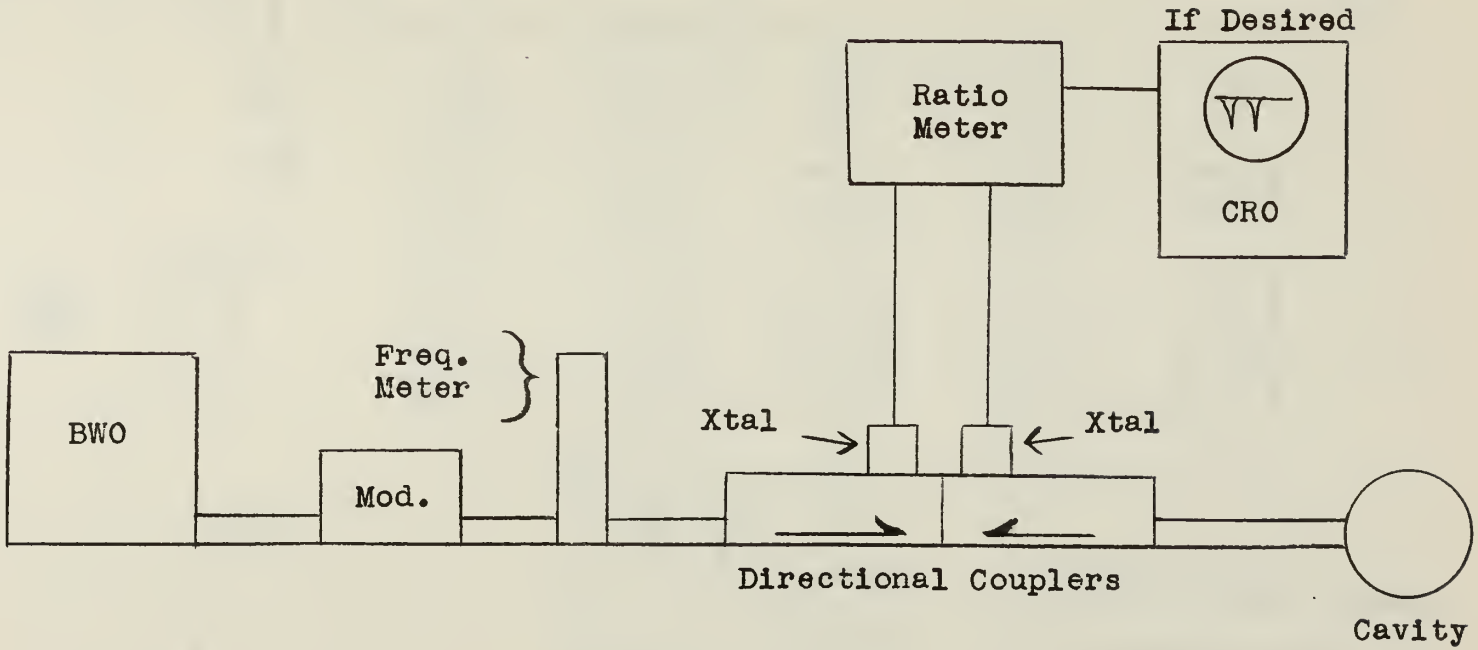

Fig. 11 Schematic of Microwave Density-Measurement Equipment

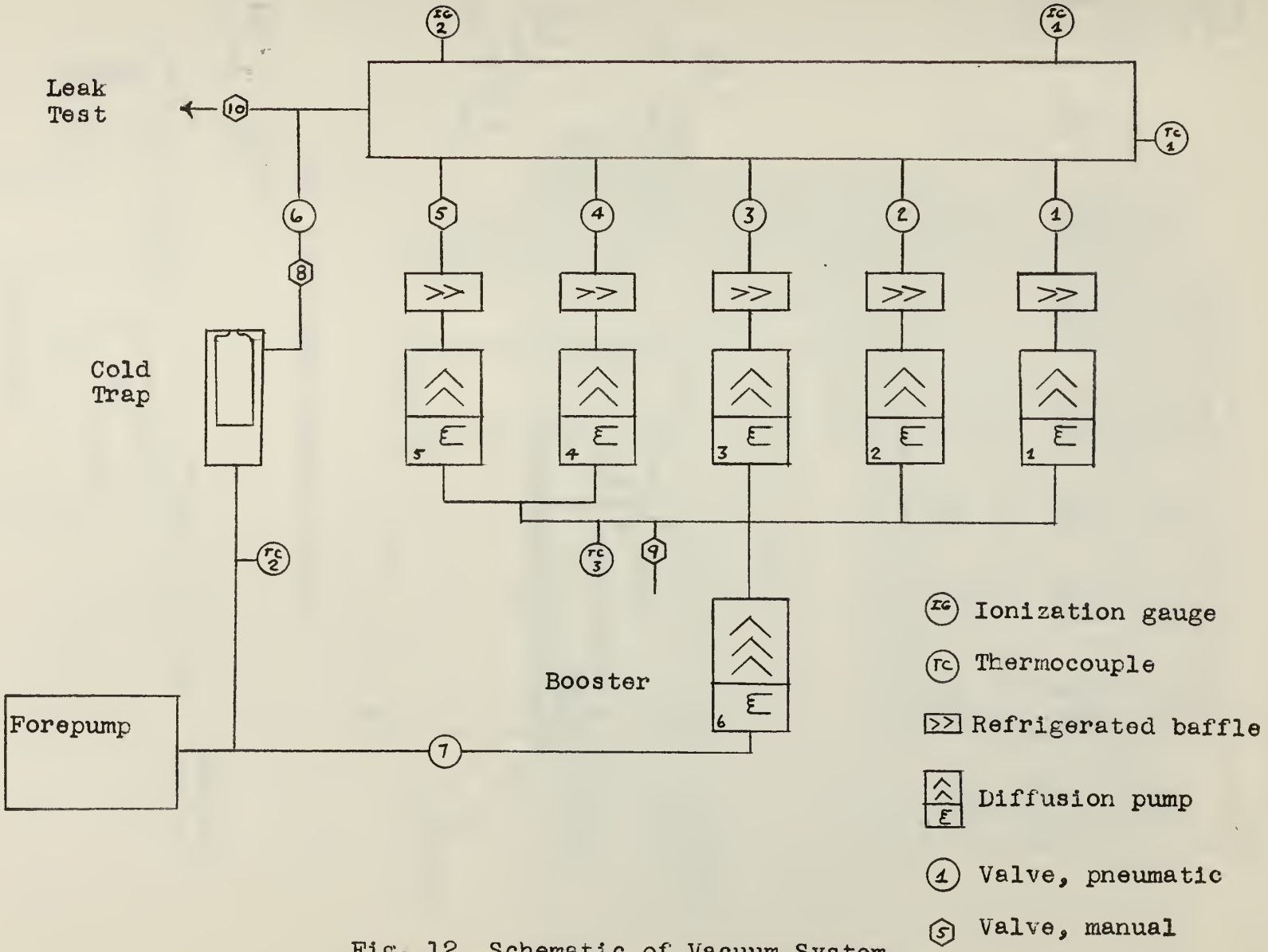

Fig. 12 Schematic of Vacuum System

Circuit Schematics

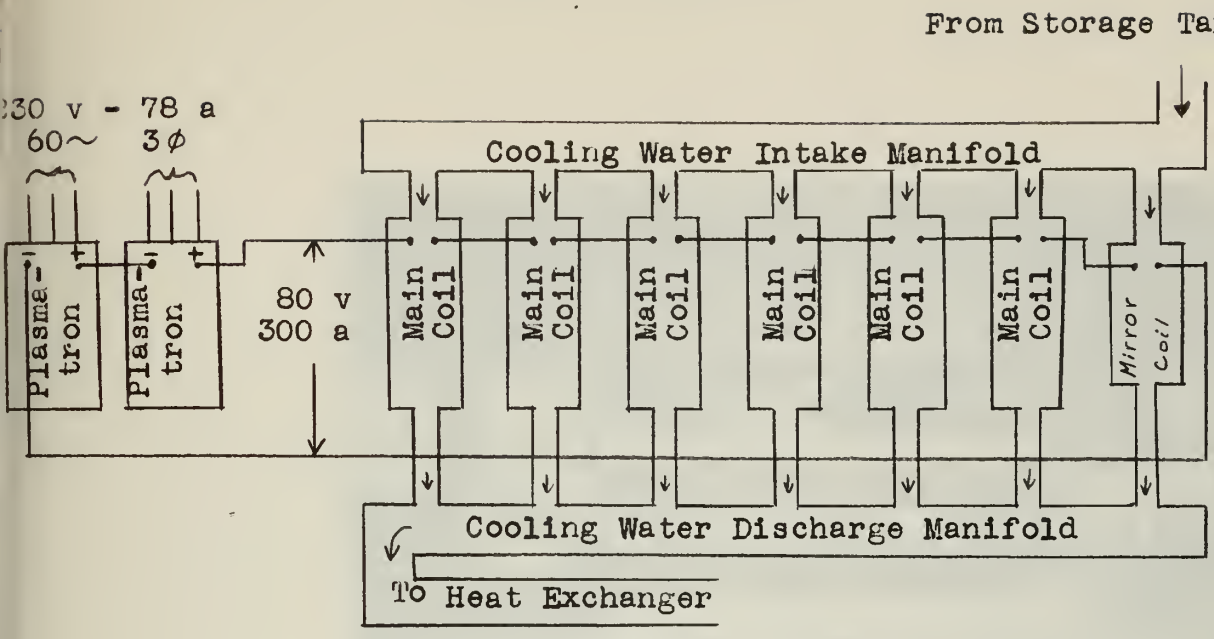

Fig. 13a Main Field Coils

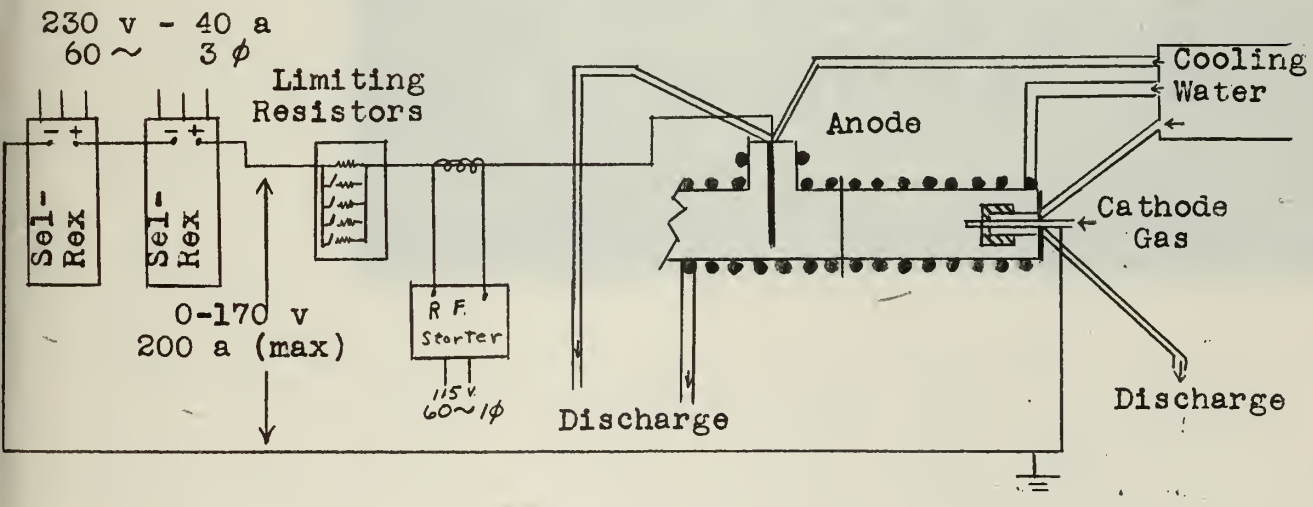

Fig. 13b Anode-Cathode Circuit

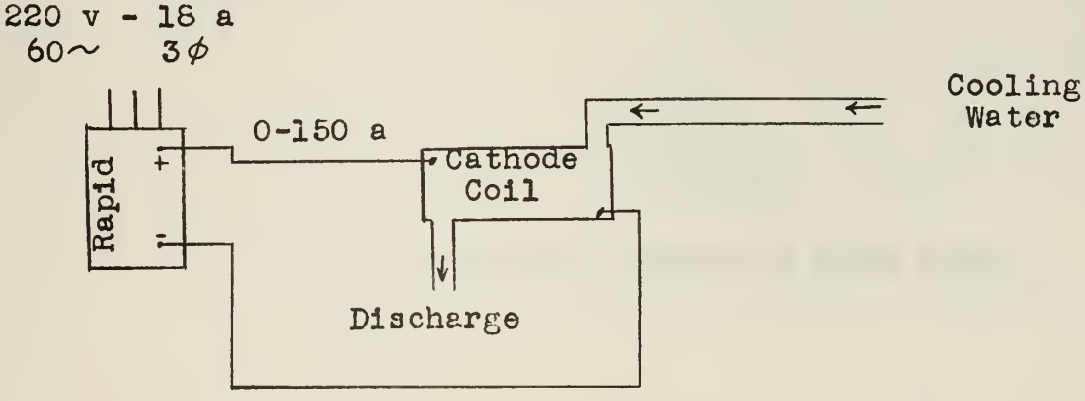

Fig. 13c Cathode Coil

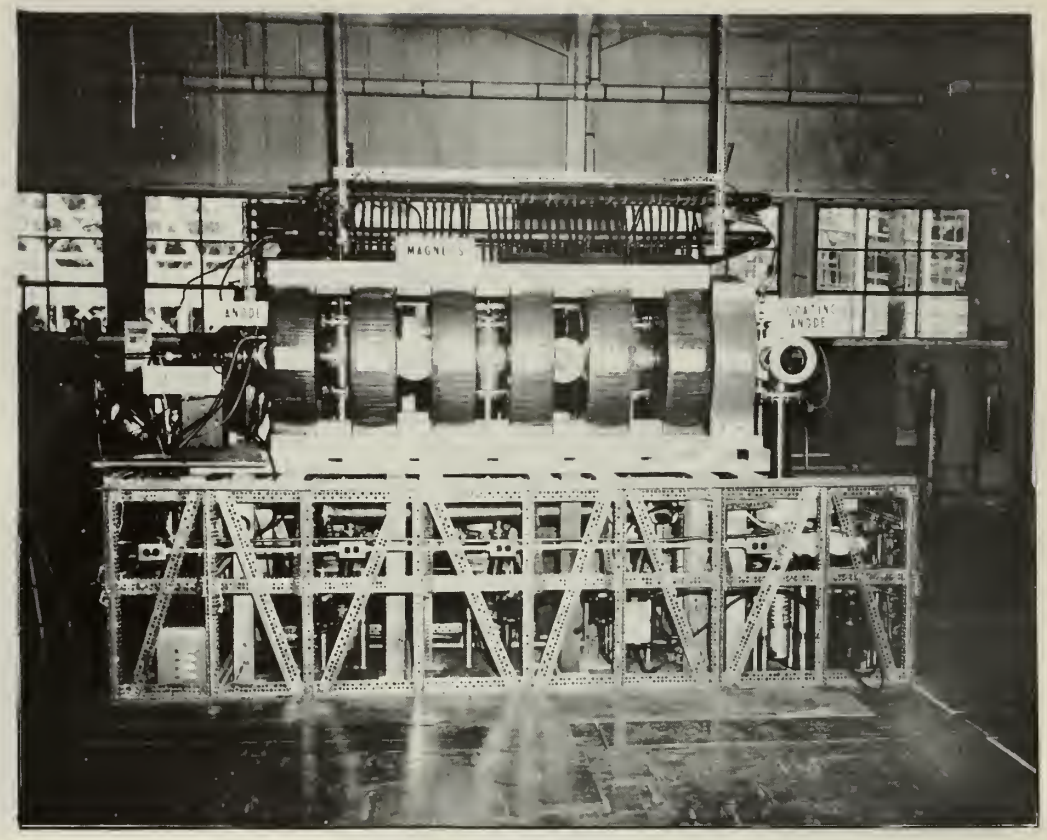

FIG 14a SIDE VIEW OF PLASMA MACHINE

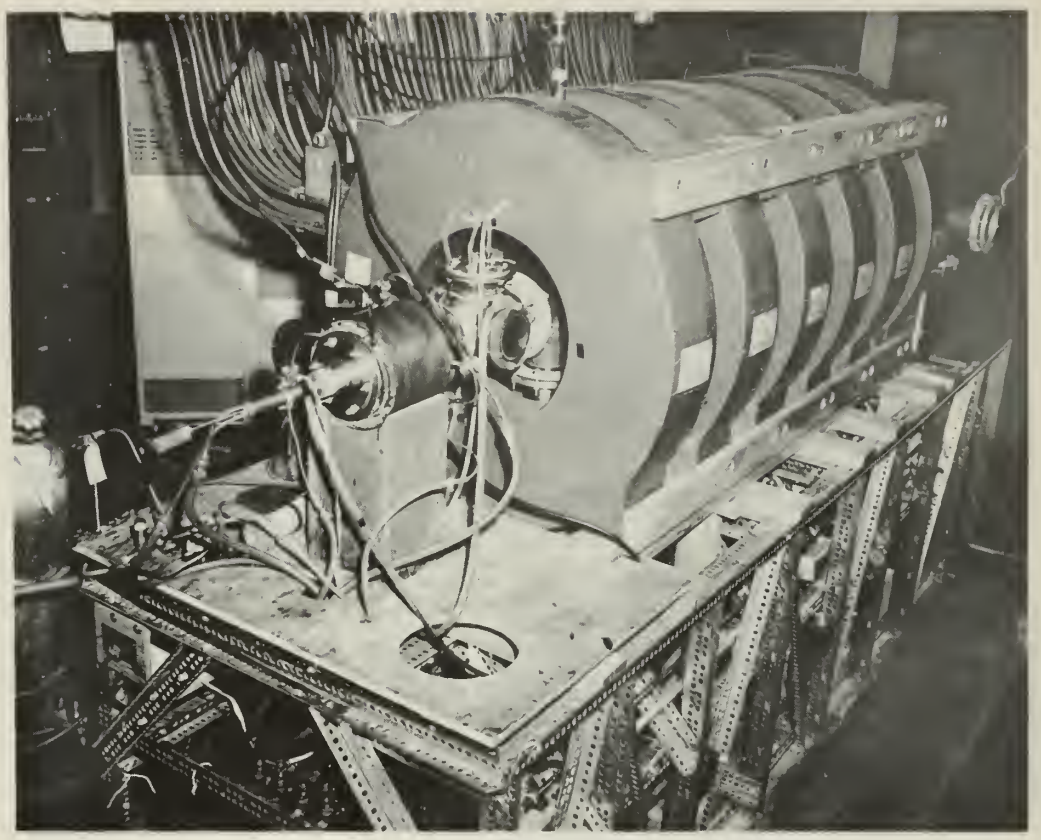

FIG 14b END VIEW OF PLASMA MACHINE SHOWING CATHODE - FIRST ANODE REGION

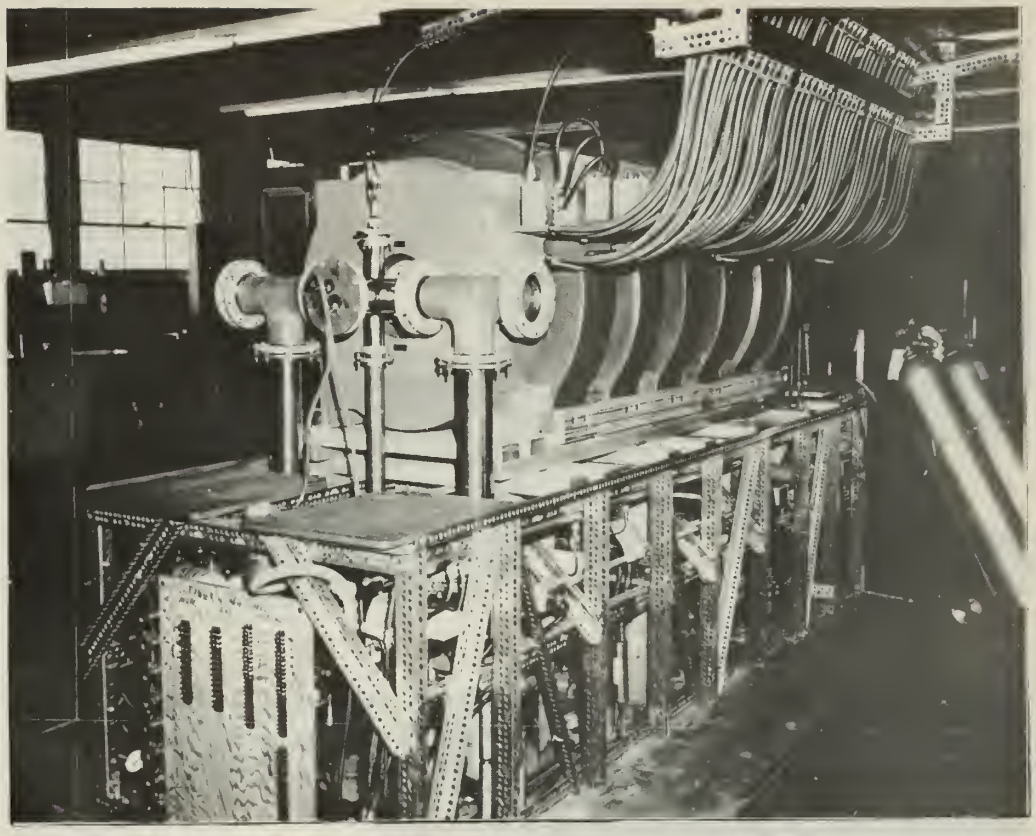

FIG 14c END VIEW OF PLASMA MACHINE SHOWING FLOATING ANODE REGION

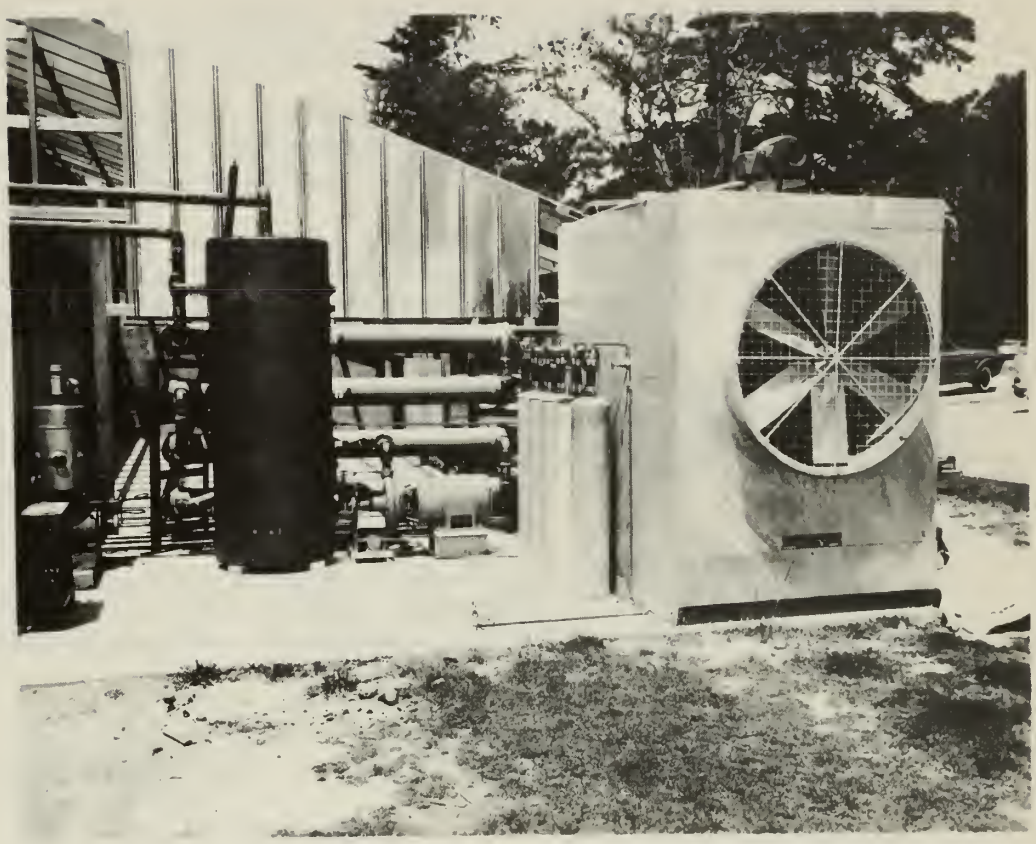

FIG 14d PHOTOGRAPH OF MAGNET COOLING SYSTEM COMPONENTS

REFERENCES

1. J. B. Streit and W. E. Olsen, Design and Construction of a Steady State Plasma Study Facility, Thesis, USNPGS, Monterey, Calif., 1962.

2. D. J. Rose et al, Highly Ionized Hollow Discharge, Preprint for Journal of Applied Physics.

3. J. S. Luce, Intense Gaseous Discharges, p. 305, Proceedings of 2nd U.N. Conference on Peaceful Uses of Atomic Energy, Vol. 31, Geneva, 1958.

4. R. V. Neigdigh and C. H. Weaver, Effects of an Applied Pressure Gradient on a Magnetically Collimated Arc, Proceedings of 2nd U. N. Conference on Peaceful Uses of Atomic Energy, Geneva, 1958.

5. N. L. Oleson, Prof. USNPGS, Conversation with U. of Calif. Plasma Group at Berkeley, Calif., approx. 1 April, 1963.

6. S. Dushman, Scientific Foundation of Vacuum Techniques, 2nd Ed., J. Wiley, New York, 1962.

7. C. D. Lustig, The Design of a TM_{010} Cavity for the Measurement of Low Plasma Densities, Project Matterhorn Microwave Memo #7, Princeton U., Princeton, N. J., Jan., 1962.

8. D. J. Rose and M. Clark, Jr., Plasmas and Controlled Fusion, MIT Press and J. Wiley, New York, 1961.

9. Veeco 400 Series Catalogue.

10. CVC Instruction Bulletin, #6-92-A.

11. NRC Equipment Corporation Installation and Operating Instructions for B-4 Booster Pump Type 126B, May, 1957.

12. Kinney Mfg. Div., Instructions 3120.8J, July, 1959.

13. Kinney Mfg. Div., Instructions Bulletin 3420.8, Nov., 1958.

14. CVC Bulletin 10-1, Nov., 1962.

15. CVC Bulletin 9-82, Nov., 1962.

16. CVC Bulletin 9-1, Nov. 1962.

17. A. Guthrie and R. K. Wakerling, Vacuum Equipment and Techniques, McGraw-Hill, New York, 1949.

18. I. Langmuir and H. Mott-Smith, General Electric Review, 27, 449, 538, 616, 762, 810, (1924).

19. I. Langmuir and H. Mott-Smith, op.-cit., p. 455.

20. A. Gardner, W. Barr, R. Kelly, N. Oleson; Diagnostic Measurements on the P-4 Steady-State Plasma-UCRL 6562, pp. 9-10.

APPENDIX A

OPERATING INSTRUCTIONS

I. To obtain a vacuum

A. From complete shutdown

1. Insure that air pressure is above 80 psi. (Gate valves #1 through #4, #6 and #7 are electrically controlled and pneumatically operated. See Fig. 12.)
2. Insure that the system is closed. (All valves closed, system components secured, etc.)
3. Turn on cooling water to forepump. (Flow rate $1\frac{1}{2}$ gallons per minute)
4. Start forepump. ((Foreline should pump down to 10 μ (TC#2) within 30 seconds.))
5. Open valve #7. ((This allows the forepump to "rough out" the D. P. section up to valves #1 through #5. This section should rough out to 25 μ (TC#3) within two minutes.))
6. Turn on baffle refrigeration. (Temperature control is automatic.)
7. Wait 30 minutes. (To allow baffles to cool)
8. Turn on cooling water to D. P.s. (.2 gallons per minute) and to the booster D. P. (.5 gallons per minute). (Insure that no cooling water is flowing to the booster D. P. boiler by positioning the cooling valve handle on the booster D. P. in the horizontal position.)
9. Apply power to all D. P.s.

10. Fill liquid nitrogen trap. (This trap prevents forepump oil vapor from backstreaming into the glass section.)

11. When the D. P. manifold pressure is below one μ (TC#3), close valve #7 and open valves #6 and #8. ((This will rough out the glass section and a pressure of 50 μ (TC#1 or TC#2) should be reached within two minutes. Valve #8 is manually operated and should be used to load the forepump gradually.))

12. When a pressure of 50 μ or less is reached, close valves #6 and #8, and open valve #7, then open valves #1 through #5. ((The D. P.s will now be pumping on the glass section, and a pressure of 5×10^{-4} mm Hg (IG1 or IG2) should be reached within three minutes. A pressure of 10^{-6} mm Hg should be reached within one hour, an ultimate lower pressure of 10^{-7} mm Hg within three hours.))

B. With glass section up to atmospheric pressure, but with D. P.s pumping up to valves #1 through #5, repeat steps 10 through 12 under section A.

II. To establish a plasma

A. Turn on all system cooling water as follows:

1. Floating anode (.5 gallons per minute)
2. First anode (.5 gallons per minute)
3. Cathode-anode shell (1.5 gallons per minute)
4. Cathode base (two gallons per minute)
5. Cathode magnet (.5 gallons per minute)

6. Cooling tower (raw water)

   a. Circulating pump (Insure that the make-up water valve is open and pressure is ~100 psi.)

   b. Fan

7. Main magnet cooling (deionized) water. (Pressure ~40 psi.)

B. Energize cathode magnet power supply to obtain a field of 200 gauss. (100 amperes, four volts d-c)

C. Energize main power supply and set desired field for starting. (~1500 gauss, 250 amperes)

D. Establish 170 volts d-c potential between cathode and first anode. (Two Sel-Rex 0-85 volts d-c, 200 ampere power supplies in series are utilized.)

E. Turn <u>off</u> all ion gauges. (RF energy to be applied in step G may damage ion gauges.)

F. Close resistor switches one through three which will limit the starting current to 130 amperes. (Resistors are provided in the arc discharge circuit which allow the current to be limited from two to 160 amperes.)

G. Turn <u>on</u> Airco starter unit to impress RF energy on the d-c arc discharge circuit.

H. Turn on argon gas valve and maintain cathode pressure $<5\mu$. (An argon plasma will now be established as described in the Arc Discharge section.)

APPENDIX B

PROTECTIVE INTERLOCKS

I. Electrical power failures.

A manually reset interlock is provided to the forepump and D. P.s to protect the system in case of a power failure. The interlock must be manually reset and the vacuum establishment procedure (Appendix A-I) followed in order to regain a vacuum after power is reestablished. Ion gauges which are re-energized will automatically cut out if their pressure range is exceeded and energized TC gauges will not be damaged at any pressure. Manually-operated valve #5 is normally closed when the system is left unattended. Since valves #1 through #4 go to the closed position when power is removed, there is no possibility of getting oil into the glass section.

II. Loss of foreline pressure.

A pressure sensing switch is provided in the foreline and is set to trip the manually reset interlock when foreline pressure exceeds 50μ. This interlock is provided to protect the system, should the forepump fail; and is normally energized when the system is unattended. Should this interlock shut off the system, the cause of the high pressure in the foreline must be corrected, and the vacuum reestablished as described in Appendix A-1.

III. Loss of water pressure

A. To D. P.s.

Each diffusion pump contains an integral thermal switch which cuts off electrical power to the boiler

until the temperature decreases to a preset safe value at which time electrical power is automatically reconnected.

B. To main field magnets.

A pressure switch is provided in the coil cooling water circuit so that if the water pressure falls below 20 psig a bell alarm is sounded, at which time the power to the coils should be secured and the cause of the low pressure investigated.

IV. Main coil cooling water temperature.

A temperature sensor is located in the cooling water discharge line and will actuate a bell alarm if the water temperature exceeds 180°F. This device will protect the coils should a cooling tower (raw water) failure occur.

APPENDIX C

VACUUM SYSTEM

COMPONENT SPECIFICATIONS AND CALCULATIONS

Component Specifications. (All components are for 4" plumbing unless otherwise specified.)

Diffusion pumps:

Three Veeco modes EP-4W three stage oil fractionating diffusion pumps charged with 200cc Dow Corning 704 silicone fluid and having a pumping speed of 400 liters/sec at .5 microns Hg. /9/.

Two CVC model PMC 721 three stage oil fractionating diffusion pumps charged with 400cc Dow Corning 704 silicone fluid and having a pumping speed of 720 liters/sec at .5 microns Hg /10/.

Booster diffusion pumps:

One NRC B-4 type 126B two stage oil fractionating diffusion pump charged with 375cc Dow Corning 702 silicone fluid and having a rated pumping speed of 50 liters/sec at 100 microns Hg /11/.

Mechanical forepump:

One Kinney KDH 130 single stage rotary piston type. Rated at 130 CFM with an ultimate base pressure of 10 microns Hg /12/.

Gate valves:

Four 4", one 6", one 2", solenoid controlled, pneumatically operated; and one 4" manually operated, Kinney Series G type. Valves close in event of loss of electric power /13/.

Baffles:

Five CVC type BC-41 multi coolant baffles (liquid nitrogen, freon, or water). Freon 12 is used giving a baffle temperature of -34.4°C which reduces backstreaming to less than 0.1% /14/.

Cold trap:

One Veeco type CT 2" stainless steel bucket /9/.

Pressure sensors:

Three ionization gauges, CVC type GK 110, using VG-1A sensing tubes with a range of one micron to 2×10^{-9} mm Hg /15/.

Three thermocouple gauges, CVC type GTC-004 /16/.

Calculations:

Throughput:

$$Q_{system} = Q_{booster} = Q_{forepump} = Q_{diffusion\ pumps} \quad (C-1)$$

The maximum throughputs of the system components are as follows:

Booster	5000 micron-liters/sec
Forepump	42000 micron-liters/sec
CVC diffusion pump	3000 micron-liters/sec
Veeco diffusion pump	2250 micron-liters/sec

Thus the booster pump limits the maximum throughput of the system to 5000 micron-liters/sec (394 atm-cc/min).

Operating pressures:

Assuming a vacuum chamber pressure of 1.7 microns and using formula /17/,

$$1/C_b = 1/S - 1/S_p \qquad (C-2)$$

C_b may be obtained for the CVC baffle from the data provided in the manufacturer's performance curves /10/. C_b = 1150 liters/sec.

Using the value of C_b and formula C-2, the speed of the Veeco-baffle combination is determined to be 291 liters/sec. Now returning to the diffusion pump performance curves, corrected for the baffle, the new throughputs are determined and their ratio is

$$\frac{Q_b \text{ - cvc dp}}{Q_b \text{ - veeco dp}} = 1.5$$

Repeating this for system pressures of 0.1 and 10 microns and averaging their throughput ratios results in:

$$\frac{Q_b \text{ - cvc dp}}{Q_b \text{ - veeco dp average}} = 1.45 \qquad (C-3)$$

From formula C-1.

Q total = $3Q_{\text{b-veeco dp}} + 2Q_{\text{b-cvc dp}}$ = 5000 micron-liters/sec

For optimum conditions, using C-3,

$Q_{\text{b-veeco dp}}$ = 850 micron-liters/sec

$Q_{\text{b-cvc dp}}$ =1230 micron-liters/sec

and going into dp performance curves /10/ gives a system pressure of three microns.

Correcting throughput for conductance in the various plumbing by use of equation C-2 and with values of conductance determined by the formula $C = .25\ D^4/l\ \bar{p}$, where D is in inches, l in feet and $\bar{p}$ in microns, or from the curve available in CVC Inst. Bull. #14-11, "The Flow of Gases Through

Vacuum Pipe Lines", permits the determination of the other system component pressures, i.e., foreline at booster, 120 microns, and booster inlet, 60 microns.

Assuming a Q = 2520 micron-liters/sec (200 atm-cc/min) which was design total-maximum-rated flow of the system.

$$Q_{\text{b-veeco dp}} = 428 \text{ micron-liters/sec}$$

$$Q_{\text{b-cvc dp}} = 620 \text{ micron-liters/sec}$$

gives a system pressure of one micron, foreline pressure of 50 microns, and a booster manifold pressure of 12 microns.

Calculations for additio al booster of same type:

$$Q_{\text{booster max}} = 5000 \text{ micron-liters/sec}$$

$$Q_{\text{booster total}} = 10{,}000 \text{ micron-liters/sec}$$

Using relative Q ratio of baffles and pumps as before one gets:

$$Q_{\text{total}} = 3Q_{\text{b-veeco dp}} + 2Q_{\text{b-cvc dp}} = 5.9\ Q_{\text{b-veece dp}}$$

$$= 10{,}000 \text{ micron-liters/sec}$$

which gives a system pressure of 12 microns.

For assumed Q of 5400 micron-liters/sec (maximum experimental Q used to date):

$$Q_{\text{b-veeco dp}} = 920 \text{ micron-liters/sec}$$

$$Q_{\text{b-cvc dp}} = 1330 \text{ micron-liters/sec}$$

which gives a system pressure of four microns.

APPENDIX D

MAGNET COOLING SYSTEM COMPONENTS AND SPECIFICATIONS

Cooling Tower:

Lilie-Hoffman Model WM 40 Redwood Tower. 77" x 60" x 80" with 2 HP 6 bladed 42" diameter fan.

Heat Exchanger:

Four American-Standard Mod 808 "HCF", 2-pass exchangers connected in series.

Storage Tank:

One A. O. Smith, permaglas, 200 gallon 150 psi tank.

Raw Water Recirculating Pump:

One Pacific Pump Co. 150 GPM, 15 HP, 3600 rpm centrifugal pump.

Main Feed Pump:

One Pacific Pump Co. Model 2M-1HU 225 GPM, 26 HP, 3540 rpm centrifugal pump.

By-pass Recirculating Pump:

One JABSCO Model 1673 6GPM, $\frac{1}{2}$ HP, 21 psi centrifugal pump.

Deionizers:

One synthetic GEL zeolite water softener.

One activated charcoal filter

Three unibed rubber-lined, anion and cation resin deionizers.

APPENDIX E

PROPOSED MODIFICATIONS

I. Interlocks: Main Field Coils.

When the main coils are operated at high currents (> 500 amperes) even momentary interruption of cooling water to them could result in rapid mechanical failure. The one temperature sensor located in the cooling water discharge line could not be expected to sense a temperature increase due to a reduced flow in one of the 42 parallel coils. For this reason, it is recommended that temperature sensors be installed on <u>each</u> coil water path outlet and that they be connected to interrupt the coil circuit should the temperature exceed 180°F. Also, the presently installed water pressure interlock should be modified to interrupt the coil circuit in place of sounding an alarm, as is presently the case.

II. Control Room.

For operation at high magnetic fields, it is desirable to provide shrapnel protection for operating personnel in case of a main coil failure. As envisioned by the authors, a control room should be constructed of .160" sheet aluminum, wherein all control panels and data recorders, less cathode gas flow, could be monitored. The mode of operation would be to establish the plasma at a low magnetic field, retire to the protected control room, and then increase the main field to the desired value; thus all personnel would be afforded maximum protection.